



HAL
open science

Improvement of semiconducting and thermomechanical properties of polymer materials based on polypyrrole and polyvinylpyrrolidone

Khaled Zeggagh, Sad Atia, Mohamed Trari, Thierry Dintzer, Christophe M elart,
Patrick L ev eque, Olivier Bardagot, Zitouni Benabdelghani

► **To cite this version:**

Khaled Zeggagh, Sad Atia, Mohamed Trari, Thierry Dintzer, Christophe M elart, et al.. Improvement of semiconducting and thermomechanical properties of polymer materials based on polypyrrole and polyvinylpyrrolidone. *Journal of Materials Science*, 2025, 60 (15), pp.6565-6580. <10.1007/s10853-025-10819-4>. <hal-05407724>

HAL Id: hal-05407724

<https://hal.science/hal-05407724v1>

Submitted on 9 Dec 2025

HAL is a multi-disciplinary open access archive for the deposit and dissemination of scientific research documents, whether they are published or not. The documents may come from teaching and research institutions in France or abroad, or from public or private research centers.

L'archive ouverte pluridisciplinaire **HAL**, est destin e au d ep ot et  a la diffusion de documents scientifiques de niveau recherche, publi es ou non,  emanant des  tablissements d'enseignement et de recherche fran ais ou  trangers, des laboratoires publics ou priv es.



HAL Authorization

Journal of Materials Science

Improvement of Semiconducting and Thermomechanical Properties of Polymer Materials Based on Polypyrrole and Polyvinylpyrrolidone

--Manuscript Draft--

| | |
|--|--|
| Manuscript Number: | JMSC-D-24-08342 |
| Full Title: | Improvement of Semiconducting and Thermomechanical Properties of Polymer Materials Based on Polypyrrole and Polyvinylpyrrolidone |
| Article Type: | Manuscript (Regular Article) |
| Keywords: | Polypyrrole(PPy) - Polyvinylpyrrolidone(PVP) - thermal and semiconducting properties - heterogeneous system. |
| Corresponding Author: | Zitouni Benabdelghani, Ph.D University of Sciences and Technology Houari Boumediene: Universite des Sciences et de la Technologie Houari Boumediene Bab Ezzouar, Algiers ALGERIA |
| Corresponding Author Secondary Information: | |
| Corresponding Author's Institution: | University of Sciences and Technology Houari Boumediene: Universite des Sciences et de la Technologie Houari Boumediene |
| Corresponding Author's Secondary Institution: | |
| First Author: | Khaled Zeggagh |
| First Author Secondary Information: | |
| Order of Authors: | Khaled Zeggagh Sad Atia, PhD Mohamed Trari, PhD Thierry Dintzer, Ph.D Christophe Mélar Patrick Lévêque Olivier Bardagot, PhD Zitouni Benabdelghani, Ph.D |
| Order of Authors Secondary Information: | |
| Abstract: | In this study, we investigate how the addition of polyvinylpyrrolidone (PVP), a thermoplastic polymer, contributes to enhance the processability, thermomechanical and semiconducting properties of a semiconducting polymer without side chains. Here, polypyrrole (PPy) is chosen as reference semiconducting polymer. Different blend ratio of PPy/PVP are prepared by in-situ polymerization in acidic solution. The pre-requisite for an effective gain in mechanical properties is to ensure an intimate mixing of both polymers. The miscibility of PPy with PVP is assessed preliminarily using thermodynamic approaches derived from the appropriate group contribution theory which is confirmed experimentally by thermal measurements using DSC and TGA, respectively. All PPy/PVP blend ratios exhibit a single glass transition temperature (T _g) characteristic of appropriate their miscibility in the solid-state. The morphology and thermal behavior of PPy/PVP mixtures is investigated by differential scanning calorimetry (DSC), and thermogravimetric analysis (TGA). The potential specific interactions between PPy and PVP moieties are investigated both qualitatively and quantitatively using FTIR spectroscopy. The FTIR study reveal specific interactions mainly hydrogen bonding between antagonist groups of PPy and PVP. The TGA analysis showed an improved thermal stability. The optical gap of PPy in the mixture PPy/PVP (0.8- 0.5 eV) determined by UV-Visible spectrophotometry is attributed to p → p* transition, while the electric conductivity measured by the four-point method |

| | |
|-----------------------------|---|
| | revealed their semiconducting behavior (57 - 3960 $\mu\text{S cm}^{-1}$). Electrochemical impedance spectroscopy (EIS) exhibits semicircles attributed to bulk material, whose diameter decreases with increasing temperature, thus confirming the semiconducting behavior of PPy; the data obey to an Arrhenius law with an activation energy of 0.1 eV and the conduction occurs by electrons delocalization through alternating double bonds. |
| Funding Information: | |

Improvement of Semiconducting and Thermomechanical Properties of Polymer Materials Based on Polypyrrole and Polyvinylpyrrolidone

Khaled Zeggagh¹, Sad Atia¹, Mohamed Trari², Thierry Dintzer³, Christophe Mélar³, Patrick Lévêque⁴, Olivier Bardagot³, Zitouni Benabdelghani*¹

¹*Macromolecular and Thiomacromolecular Chemistry Laboratory, Faculty of Chemistry, University of Sciences and Technology (USTHB), BP 32, El Alia, Algiers 16111, Algeria*

²*Laboratory of Storage and Valorization of Renewable Energies, Faculty of Chemistry, University of Sciences and Technology (USTHB), BP 32, El Alia, Algiers 16111, Algeria.*

³*Institute of Chemistry and Processes for Energy Environment and Health (ICPEES), University of Strasbourg, CNRS, 25 rue de Becquerel, 67087 Strasbourg, France*

⁴*Laboratoire des Sciences de l'Ingénieur, de l'Informatique et de l'Imagerie (ICube Research Institute), University of Strasbourg, CNRS, 23 rue du Loess, 67037 Strasbourg, France*

* To whom all correspondence should be addressed (zitouni.benabdelghani@usthb.edu.dz)

Received [Dates will be filled in by the Editorial office]

Abstract

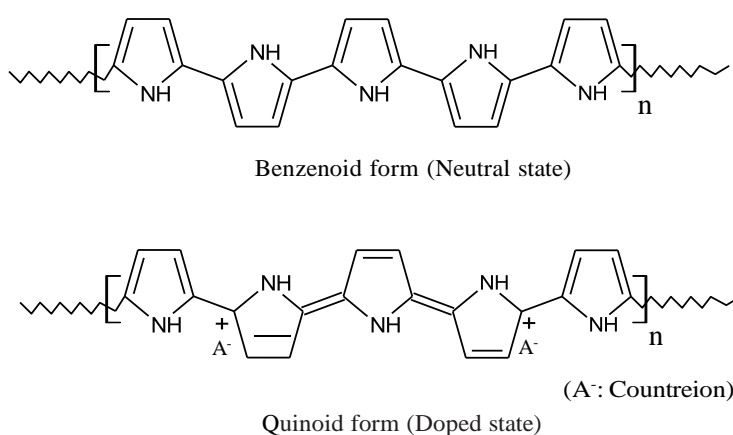
In this study, we investigate how the addition of polyvinylpyrrolidone (PVP), a thermoplastic polymer, contributes to enhance the processability, thermomechanical and semiconducting properties of a semiconducting polymer without side chains. Here, polypyrrole (PPy) is chosen as reference semiconducting polymer. Different blend ratio of PPy/PVP are prepared by in-situ polymerization in acidic solution. The pre-requisite for an effective gain in mechanical properties is to ensure an intimate mixing of both polymers. The miscibility of PPy with PVP is assessed preliminarily using thermodynamic approaches derived from the appropriate group contribution theory which is confirmed experimentally by thermal measurements using DSC and TGA, respectively. All PPy/PVP blend ratios exhibit a single glass transition temperature (T_g) characteristic of appropriate their miscibility in the solid-state. The morphology and thermal behavior of PPy/PVP mixtures is investigated by differential scanning calorimetry (DSC), and thermogravimetric analysis (TGA). The potential specific interactions between PPy and PVP moieties are investigated both qualitatively and quantitatively using FTIR spectroscopy. The FTIR study reveal specific interactions mainly hydrogen bonding between antagonist groups of PPy and PVP. The TGA analysis showed an improved thermal stability. The optical gap of PPy in the mixture PPy/PVP (0.8- 0.5 eV) determined by UV-Visible spectrophotometry

34 is attributed to $\pi \rightarrow \pi^*$ transition, while the electric conductivity measured by the four-point method revealed their semiconducting behavior ($57 - 3960 \mu\text{S cm}^{-1}$). Electrochemical impedance spectroscopy (EIS) exhibits semicircles attributed to bulk material, whose diameter decreases with increasing temperature, thus confirming the semiconducting behavior of PPy; the data obey to an Arrhenius law with an activation energy of 0.1 eV and the conduction occurs by electrons delocalization through alternating double bonds.

Keywords: Polypyrrole(PPy), Polyvinylpyrrolidone(PVP), thermal and semiconducting properties, heterogeneous system.

Introduction

The organic semiconductors are among the most and pertinent fields of research which continue to attract much attention to improve their physical and chemical properties. They are used in the solar energy conversion under various forms [1] and have many attractive properties like ease of synthesis, moderate electrical conductivity and thermal and chemical stability in their oxidized form. In this context, PPy is among the most extensively studied semiconducting polymers. Due to its intrinsic properties, it is a potential candidate as supercapacitors, batteries, biosensors and solar energy [2]. Structurally, PPy is more compact than polyaniline (PANI), and its linear structure contributes to its rigidity, which limits its applicability in various fields. Previous studies reported that PPy has a better thermal stability and electrical conductivity compared to doped (PANI). As shown in scheme 1, the presence of nitrogen in the polypyrrole structure allows specific interactions with a suitable thermoplastic matrix.



Scheme 1. The neutral and doped forms of PPy.

67 It has been admitted that the nanostructured polypyrrole gives the obvious advantages over its
bulk structured. Very recently, Y. Demei and co-workers have studied polypyrrole
nanomaterials where they have focused mainly their interest on three aspects such as structure,
properties and preparation of polypyrrole nanomaterials. They have concluded that controlling
the size and morphology of PPy nanomaterials is still a major challenge in this field [3].

Previously, we have studied the semiconducting and photochemical properties of PPy [4]. and
found that the conduction band is appropriately positioned with respect H_2O/H_2 level, yielding
spontaneous hydrogen evolution reaction [5]. The doped polypyrrole can be obtained easily by
chemical synthesis. However, the strong interchain interactions within the backbone of chain
and the presence of conjugated double bonds make these conductive polymers infusible and
insoluble in most organic solvents. Furthermore, due to this strong rigidity, these polymers
exhibit poor mechanical properties, making the electrochemical characterization difficult to
undertake.

To remedy this issue and enhance their properties, various methods have been proposed. One
significant approach is blending of semiconducting polymers with suitable thermoplastic poly-
mers, which represents a promising avenue for developing new organic semiconductors through
in situ polymerization. This method is widely adopted and is regarded as both effective and
cost-efficient. [6, 7].

Polyvinylpyrrolidone (PVP) is among the most studied thermoplastic polymer. It is an inter-
esting linear polymer with a broad range of industrial applications. The presence of carbonyl
groups in the structure of PVP is particularly interesting since it can be used to develop specific
interactions with amine and imine groups of PPy. Thus, owing to advantageous characteristics,
like its adhesiveness to various substrates, film formation property, and solubility in water, PVP
can be applied in a variety of fields such as cosmetics, pharmaceutical and electronic [8,9].

In this contribution, we have firstly assessed thermodynamically the possibility to blend PPy
with PVP using the group contribution model to calculate the solubility parameters of both
polymers. Our main goal is to combine two types of polymers, conductor and insulator, in order
to produce the semiconducting materials possessing improved properties with large scale ap-
plications. The binary system blend PPy/PVP are obtained by in-situ polymerization and stud-
ied by means of DMA and DSC analysis, FTIR spectroscopy and thermogravimetry (TGA).
99
100 Their electrical conductivity and gap energy were measured by the four-point technique and

101 UV-Visible spectrophotometry respectively. The phase behavior and miscibility of these blends were examined according to their glass transition temperature (T_g). Moreover, the specific interactions, mainly hydrogen bonds, were studied qualitatively and quantitatively by FTIR spectroscopy. The X-ray diffraction (XRD), thermal stability and conductivity properties of these materials were also explored. The electrochemical properties of doped PPy were determined by EIS analysis.

108 **Experimental**

19 *Materials*

109 PVP with an average molecular weight of 40000 g/mol is purchased from Sigma Aldrich and
110 used without any further purification. Doped PPy is obtained by chemical oxidation using molar
111 ratios of HCl/pyrrole = 1.5 and $(\text{NH}_4)_2\text{S}_2\text{O}_8$ /pyrrole = 1.15.
112

113 *Pure PPy and PPy/PVP blend film fabrication*

114 1 mL of pyrrole is added in the required amount of a HCl solution under stirring for 30 min.
115 3.79 g of $(\text{NH}_4)_2\text{S}_2\text{O}_8$ dissolved in distilled water is added dropwise to the solution. The
116 polymerization was carried out under magnetic agitation at 273 K. The resulting dark green
117 PPy powder is then filtrated and rinsed distilled water and ethanol to eliminate the traces of acid
118 and oligomers. The obtained polypyrrole powders is dried under primary vacuum for several
119 days.
120

Thus, PPy/PVP mixtures at different ratios were obtained by in-situ polymerization in the same conditions as mentioned above for pure PPy.

To prepare PPy/PVP films, different amounts of PVP are dissolved in methanol. An appropriate quantity of pyrrole and HCl (1 M) are added to the PVP solution. The resulting mixtures were stirred 1 h to ensure a better dispersion of pyrrole in the PVP polymer matrix. The polymerization is then initiated by a dropwise addition of the $(\text{NH}_4)_2\text{S}_2\text{O}_8$ solution. Blends of PPy/PVP are finally obtained by solution casting in a Teflon disk, dried in the open air for several days and in oven at 303 K for 48 h. The polymerization conditions of PPy and PPy/PVP are summarized in Table 1.

The glass temperature (T_g) of two polymers and of their binary blends was measured with a TA Instruments DSC 25 equipped with an intercooler and TA Instruments DMA DHR Series. The measurements were carried out at a heating rate of 20 °C/min under N_2 flow and the T_g value was taken as the midpoint of the transition of the second scan.

FTIR measurement was carried out with a Nicolet iS10 FTIR spectrometer where 32 scans were collected with a spectral resolution of 2 cm^{-1} in ATR mode. The spectra of the PPy, PVP and their mixtures were obtained on the films prepared by casting in Teflon disks. All the samples were dried to constant weight under vacuum oven at 50 °C for several days to evaporate slowly the solvent.

DMA measurements were performed in a bending mode over the temperature range from -50
140 to 200 °C. Data acquisition and analysis of the storage modulus (E'), loss modulus (E''), and

141 loss factor ($\tan \delta$) were recorded. The heating rate and frequency were fixed at 3 °C/min and 1
1 Hz, respectively.

TGA was carried out under N₂ atmosphere using a Mettler Toledo TGA2 with a heating rate of 10 °C/min.

X-ray diffraction was performed with a Malvern Panalytical diffractometer using a CuK α anti-cathode ($\lambda = 0.154$ nm) in the 2θ range (5 - 60°).

The UV-Visible spectrophotometry of solids was carried out with a Jasco V-650 over the λ -range (190 - 900 nm) with BaSO₄ as reference.

The electrical conductivity was measured under controlled atmosphere in a glove box using the four Point Probe Stand KSR-4. To avoid free humidity measurement, a primary pump allows the vacuum to be lowered down to ~ 0.1 mbar, then N₂ gas was introduced at 1 atm, this operation was performed 3 times and the same procedure was repeated for each measurement.

The impedance spectroscopy (IS) was performed using an Autolab 302N Potentiostat / Galvanostat coupled to a Microcell HC temperature controller between 25 and 95 °C. The compacted pellet was sandwiched between two stainless steel electrodes and the measurements during cooling, making the measurement more reliable; each point was stabilized within 30
158 min. The frequency range was set from 0.1 MHz to 0.1 Hz and 10 mV amplitude.

159

| Composition of Pyrrole/PVP | Pyrrole (mL) | HCl 1M (mL) | (NH ₄) ₂ S ₂ O ₈ (g) | PVP (g) |
|-------------------------------|-----------------|----------------|--|------------|
| 1/0 | 1 | 21.68 | 3.79 | - |
| 1/1 | 0.5 | 10.84 | 1.90 | 0.61 |
| 1/2 | 0.5 | 10.84 | 1.90 | 1.21 |
| 1/5 | 0.5 | 10.84 | 1.90 | 3.03 |
| 1/10 | 0.5 | 10.84 | 1.90 | 6.06 |
| 1/20 | 0.2 | 4.33 | 0.76 | 4.84 |

160 **Table 1.** Polymerization conditions of pure PPy and PPy/PVP blend at different ratios.

161

162

163

164

49
50
51
52
53
54
55
56
57
58
59
60
61
62
63
64
65

1. Thermodynamic Study

As emphasized earlier, polymer blending is an attractive approach for obtaining new polymeric materials with desired properties. This process is an effective alternative for achieving enhanced material properties with improved processability and reduced costs. Thus, it is well-known that the miscibility of polymer blends primarily depends on the mixing enthalpy, as the contribution of mixing entropy is negligible. Consequently, the selection of polymer moieties is primarily assessed based on thermodynamic considerations. Generally, to achieve a miscible blend system, it is necessary to ensure the presence of favorable specific interactions between the components. In this context, various methodologies and strategies have been developed to enhance the thermomechanical properties of semiconducting polymer materials. Among these methods, the blending technique using the thermoplastic polymers as matrices, capable of incorporating semiconducting materials, has gained increasing importance and is regarded as one of the most economical approaches to achieve complete miscibility. However, it has been suggested that blending two polymers can be accomplished in different ways.

The first method involves mixing PPy with PVP in a common solvent, such as ethanol. However, this approach typically results in a heterogeneous system. Alternatively, the second method entails synthesizing PPy on a thermoplastic polymer matrix through an in-situ polymerization process. As shown in scheme 2, this approach is considered the most effective for producing homogeneous materials.

204 limited, requiring the use of theoretical approaches. Therefore, group contribution theory is considered one of the most reliable methods for predicting these parameters.

The solubility parameter model has been successfully applied to polymer solutions, particularly when the liquid components are non or slightly polar, where their interactions are dominated by dispersion forces. Therefore, as the entropic contribution in polymer blends is usually negligible, it is generally accepted that two polymers are miscible if their solubility parameters are similar. This criterion is qualitatively used as a key factor to describe the miscibility of PPy with PVP.

Knowledge of the solubility parameters and/or surface tension parameters using group contributions can also be used to predict some physical properties of polymers and their blends. In this context, some approaches have been proposed to predict the solubility parameter of components (δ_i). Among them, the Hoftyzer and Van Krevelen method is the most reliable, especially when specific interactions are present within different species. For this purpose, δ_i is related to the of vaporization heat (ΔH_{vap}) and the molar volume of liquid (V_i) by [11]:

$$\delta_i = \left(\frac{E_{coh}}{V_i} \right)^{1/2} = \left(\frac{\Delta H_{vap} - RT}{V_i} \right)^{1/2} \quad (2)$$

For a system involving specific interactions such as hydrogen bonding and/or ionic interactions, Hansen has considered that the total cohesive energy (E_{coh}) is the contribution of three types of interaction forces given by:

$$E_{coh} = E_d + E_p + E_h \quad (3)$$

where E_d , E_p and E_h are the contribution of dispersion forces, polar forces and hydrogen bond, respectively.

Dividing the two sides of equation (3) by the molar volume gives the square of the total solubility parameter:

$$\delta_t^2 = \delta_d^2 + \delta_p^2 + \delta_h^2 \quad (4)$$

49 where δ_t as the sum of the squares of the dispersion (δ_d), polar (δ_p), and hydrogen bonding
50
51
52
231 (δ_h) components.

53
54
55
232 According to Hoftyzer and Van Krevelen method, the total solubility parameter may be esti-
56
233 mated from group contributions based on the following equations:

57
58
59
60
61
62
63
64
65
234

$$\delta_d = \frac{\sum F_d}{V}; \quad \delta_p = \frac{\sqrt{\sum F_p^2}}{V}; \quad \delta_h = \sqrt{\frac{\sum E_h}{V}} \quad (5)$$

which F_d , F_p , and E_h are the contributions of the dispersion force, the polar forces, and the hydrogen bond force, respectively.

The predicted solubility parameters of PPy and PVP, using appropriate group contributions are given in Table 2. As observed, the solubility parameters of the two polymers calculated using the appropriate group contribution model, align with values reported in the literature [11].

The solubility parameter of PPy is very close to that of PVP, with a difference between them of ($\Delta\delta_{max}$) not exceeding 0.42. suggesting that the two polymers may be completely miscible. According to the mean field theory, this value indicates that the interactions between PVP and PPy groups are relatively moderate, consistent with the conclusions drawn by Coleman et al [12]. The presence of antagonistic groups, such as carbonyl, imine, and amine groups within the species, can be regarded as precursors for enhancing specific interactions.

Table 2 Predicted solubility parameters of PVP and PPy using group contributions theory

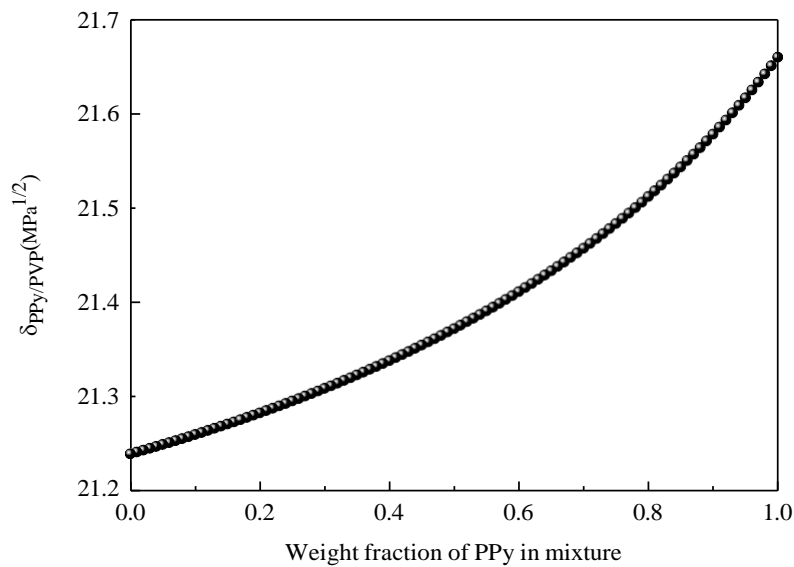
| Polymers | δ_t | δ_d | δ_p | δ_h |
|----------|------------|------------|------------|------------|
| PVP | 21.24 | 15.50 | 11.70 | 08.60 |
| PPy | 21.66 | 19.50 | 04.60 | 08.24 |

Assuming the additivity rule of the solubility parameters of both polymers, one can calculate the solubility parameter of each ratio of the PPy/PVP blend across the entire composition range using the following expression [10]:

$$\delta_{PPy/PVP} = \Phi_{PPy}\delta_{PPy} + \Phi_{PVP}\delta_{PVP} \quad (6)$$

where Φ_i and δ_i are the volume fraction and solubility parameter of each polymer, respectively.

261 The predicted solubility parameter of the mixture PVP/PPy plotted against the weight fraction
262 of PPy is displayed in Fig. 1. The slight negative deviation from the additivity rule is observed
263 with these blends, suggests the presence of specific interactions between PVP and PPy. Thus,
264 it might be noted that the trend of this evolution generally indicates that the two polymers PPy
265 and PVP are completely miscible over the entire range of composition where $\Delta\delta_{\text{PPy/PVP}}$ is less
266 than or equal to 0.42.



278 **Fig. 1** Evolution of predicted solubility parameter versus PPy weight fraction in mixture
279 PPy/PVP.

280 2. DSC Study

281 To further confirm this theoretical finding, the thermal measurements are conducted on pure
282 PVP and the mixtures PPy/PVP. It is important to note that due to the compact structure of PPy,
283 determining its glass transition temperature is challenging. Nevertheless, theoretical methods
284 based on group contributions theory were employed to estimate it [11].

285 The transition phenomena observed in polymers serve as a fundamental criterion for studying
286 the miscibility of polymer blends. In particular, glass transition phenomena provide valuable
287 insights into the physical state and morphology of these blends. They reveal various relaxation
288 processes and possible orientations occurring at the chain segment level during the transition.

290 Differential scanning calorimetry (DSC) is one of the most widely used techniques for studying
291 these phenomena. It is a vital tool, providing rapid and reliable results for characterizing the
292 physical state, morphology, and chain orientation of polymers.

1
2
3
4
5
6
7
8
9
10
11
12
13
14
15
16
17
18
19
20
21
22
23
24
25
26
27
28
29
30
31
32
33
34
35
36
37
38
39
40
41
42
43
44
45
46
47
48
49
50
51
52
53
54
55
56
57
58
59
60
61
62
63
64
65

293 In this study, we have employed DSC to investigate the PPy/PVP system. In this context, ob-
294 serving a single glass transition temperature (T_g) in such blends can indicate either an interme-
295 diate value between the T_g values of the two components or a significantly higher T_g compared
296 to both polymers. The latter case is often associated with blends exhibiting strong specific
297 interactions, such as hydrogen bonding or dipole-dipole interactions. The presence of a homo-
298 geneous phase in the binary blend can be considered a key criterion for assessing miscibility. On
299 the other hand, the detection of two T_g corresponding to the pure constituents, with the obser-
300 vation of two or more phases is indicative of their immiscibility.

301
302 Poly(pyrrole) (PPy) is composed of conjugated motifs, making the determination of its glass
303 transition temperature (T_g) rather challenging. Consequently, the group contributions method
304 appears to be a reliable approach for estimating its T_g . In order to determine the glass transition
305 temperature of PPy, we employed the Van Krevelen and Hoftyzer method, which is based on
306 the additivity rule of structural groups as expressed in the following equation: [12]

$$Y_g = \sum Y_{gi} = T_g M \quad (7)$$

307
308 where Y_{gi} is the specific contribution to a given structural group, and $T_g M$ is called molar glass
309 transition function. Using this approach, the calculated glass transition temperature of PPy was
310 found to be 110 °C, which aligns well with those reported in the literature [13].

311
312 The DSC profiles of PPy/PVP blends (Fig. 2) revealed the presence of a single T_g specific to
313 each composition. Although PPy does not exhibit a clear transition in this DSC analysis, prob-
314 ably because of its rigid structure, its combination with PVP in various ratios has resulted in
315 transitions indicating that the structures of the developed materials have become flexible. In-
316 deed, a single intermediate T_g indicates that the studied blends are miscible. Therefore, these
317 results indicate that this miscibility is attributed to the presence of specific interactions such as
318 hydrogen bonding that can occur between both two carbonyl groups of PPy and PVP, respec-
319 tively.

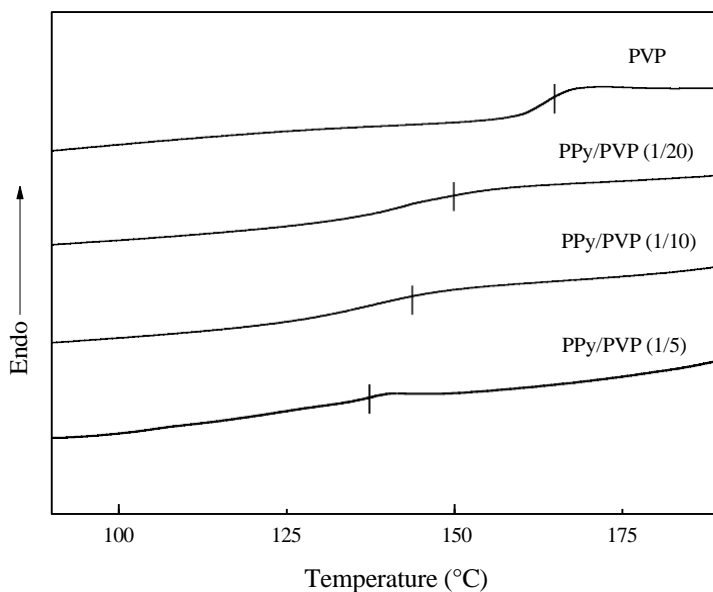


Fig. 2 DSC thermograms of PPy, PVP and their different mixtures.

3. DMA Study

The presence of phenyl groups along the PPy chain significantly affects its elasticity, making the detection of the glass transition temperature using DSC more difficult. For this reason, we have additionally used DMA measurements to provide supplementary information about the homogeneity of the structure of PPy/PVP materials and to verify the possible relaxations occurring at the segment level during the transition. In this context, DMA analysis is more sensitive than any other thermal analysis technique, particularly for determining T_g and detecting transitions of polymers. Fig. 3 illustrates the loss factor ($\tan \delta$) of PPy, PVP, and their blends in different ratios. As can be seen, the relaxation behaviors of the samples are observed, reflecting the mode of chains motion in the amorphous region. This corresponds to the maximum of $\tan \delta$, attributed to the glass transition temperature (T_g), which increases with increasing the PVP content in the mixture. Thus, it should be noted that all mixtures revealed one T_g between those of the pure constituents PPy and PVP. Also, the obtained T_g values using DMA measurements are very close to those obtained by DSC study. The small level of $\tan \delta$ observed with doped PPy may be due to low relaxation reflecting its higher crystallinity and, therefore, its rigidity.

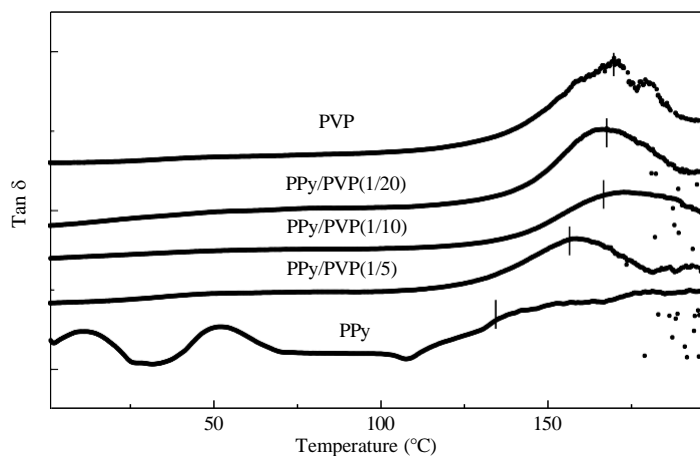


Fig. 3 Loss factor vs temperature of mixtures PPy/PVP in different ratios

4. FTIR Study:

The presence of different chemical groups in polymer blends often leads to various types of repulsive and/or attractive interactions. For this reason, FTIR spectroscopy commonly used to explore such interactions, was undertaken. It is a powerful technique for studying specific interactions, particularly for detecting hydrogen bond. However, it has been suggested that hydrogen bonds significantly affect covalent bonds on interactive species, which a frequency shift. The FTIR carbonyl-carbonyl stretching range is sensitive to the formation of hydrogen bonds. It should be noted that this region is particularly important because PVP absorbs and not PPy.

Firstly, we focused on the FTIR analysis of the two polymers and their blends. The primary objective is to identify the characteristic bands related to the functional groups present within the basic structures, and subsequently, detect any potential change and/or shift in these characteristic bands when the two polymers are blended. Additionally, the specific hydrogen bonds interactions may occur between the carbonyl groups of PVP and those of PPy, and then on their quantification as a function of PVP composition in the blend.

As mentioned above, the first step is devoted to the qualitative study of the overall spectra of PVP and PPy, in order to assign the bands related to the functional groups. Indeed, the regions of interest that could serve as references in this spectroscopic study are the regions...

Fig. 4 displays the global FTIR spectra of PVP and PPy. Although PPy does not absorb in the carbonyl and hydroxyl regions, it presents characteristic bands in the phenyl and amine/imine regions. Examination of the overall spectrum of PPy reveals several bands that can serve as references in our spectroscopic study.

393 The spectrum of PPy shows two bands centered at 1553 and 1459 cm^{-1} , corresponding to the
394 stretching vibration of the double bond C=C and C-N of pyrrole cycle respectively, which de-
395 pends directly on the degree of electron π delocalization and doping of PPy [13]. Additionally,
396 the two bands observed at 1292 and 915 cm^{-1} are attributed to the deformation vibration of =C-
397 H, in perfect agreement with the literature [14].

399 The spectrum of PVP has two principal bands localized in C=O and O-H regions, characterizing
400 the different groups existing in this polymer. The broad band at 3400 cm^{-1} is assigned to the
401 elongation of the associated OH...O mainly due to the existence of hydrogen bonding between
402 the PVP carbonyls and H₂O, confirming the high hygroscopy of PVP. The intense band at 1652
403 cm^{-1} is attributed to the stretching vibrations of the free carbonyl groups of PVP.

405 On the other hand, several bands are also observed in the region (1245-1520 cm^{-1}). The band
406 appeared at 1443 cm^{-1} is due to the stretching of -(N-C)=O while the band at 1292 cm^{-1} , is
407 attributed to the stretching vibration of -(C-N)-C.

408 It should be noted that the doped PPy does not absorb in carbonyl and in hydroxyl regions but
409 has rather characteristic bands in the phenyl and amine / imine region. In addition, the global
410 spectrum of PPy shows several bands that can serve as reference in this spectroscopic study.

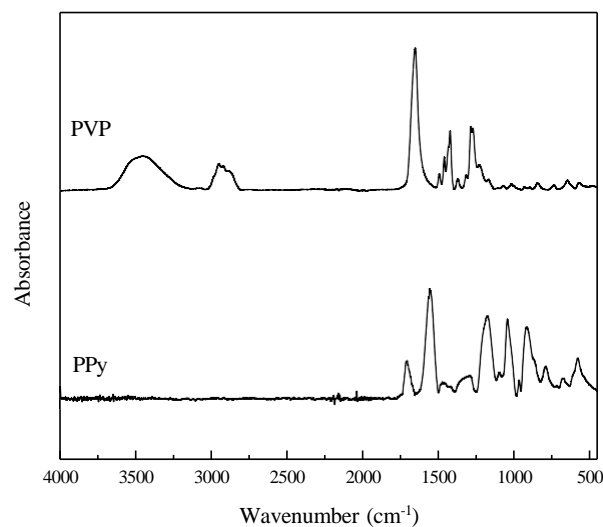


Fig. 4 FT-IR spectra of PVP and PPy in the 400–4000 cm^{-1} region.

423 As mentioned above, due to its high sensitivity, the FTIR spectroscopy is particularly suitable
424 for the elucidation of specific interactions, in particular the hydrogen bond. In general, the pres-
425 ence of groups of different chemical nature within the polymer mixtures often induces several
426 types of repulsive and attractive interactions.

427

428 In this part, we have firstly focused our interest on the demonstration of the specific interactions
429 hydrogen bond type that take place between the C=O groups of PVP and the amine / imine
430 groups of the doped PPy, and their quantification depends on the composition of PVP in the
431 mixture.

432

433 The first step is devoted to the qualitative study of the specific interactions of the hydrogen
434 bond present in the different PPy / PVP binary mixtures in the fields of interest. The effective-
435 ness of this technique has been proven in the polymer mixtures, particularly when one of the
436 constituents is absorbed and the other is not. As can be seen, PVP absorbs in the stretching
437 carbonyl region unlike PPy, which is a further advantage to spectroscopic study in this region.
438 Although PPy does not absorb in hydroxyl region ranging from (3100 - 3500 cm^{-1}), which is
439 relatively complex since PVP is considered among the potential hygroscopic polymers.

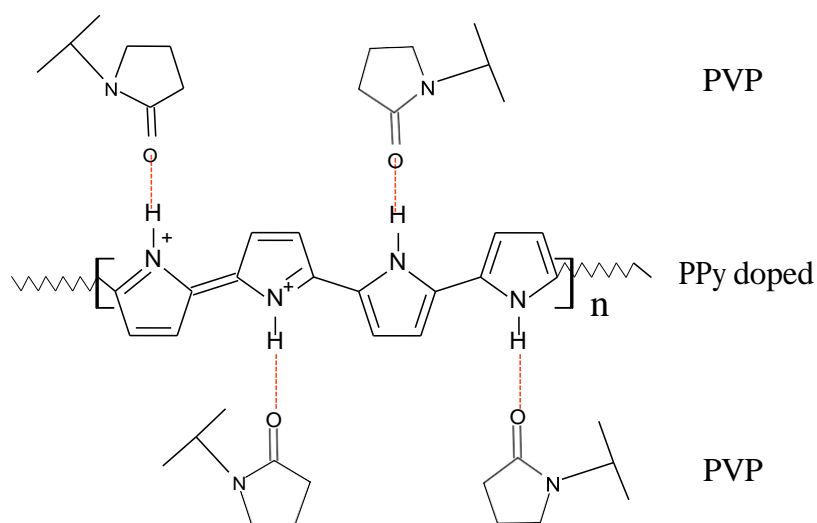
440 According to the chemical structures PPy and PVP, the expected specific interactions within
441 the PPy/PVP systems are illustrated in scheme 3.

442

443

444

445



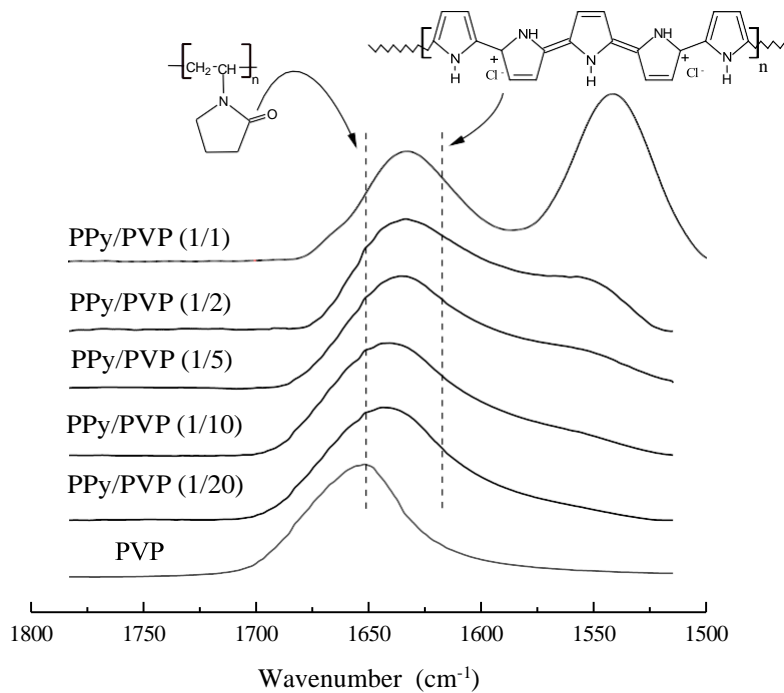
455

456 **Scheme 3:** Potential specific interactions involved on PPy/PVP systems

457

458 For this purpose, two regions of interest were selected for the characterization of the different
459 carbonyl-amine and carbonyl-imine interactions. On the other hand, the C=O stretching region
460 (1600-1780 cm^{-1}) is important because the doped PPy is transparent and show no absorptivity

461 in the C=O region, whereas PVP has one characteristic band observed at 1652 cm⁻¹ correspond-
 462 ing to free carbonyl. It is important to note that when the amount of PVP is progressively added
 463 to the doped PPy in the mixture, the characteristic band shifts progressively to a lower frequency
 464 stretching mode up 1633 cm⁻¹(Fig. 5). This important shift may be attributed to the increased
 465 rigidity of the PVP rings, serving as evidence of hydrogen bonding between PVP and PPy.
 466 Besides, we observe the apparition of the second band localized at 1620 cm⁻¹ assigned to the
 467 hydrogen bond in the mixture. Therefore, as two type of specific interactions carbonyl-amine
 468 and carbonyl-imine have approximately the same forces and consequently their characteristic
 469 bands could overlap [15, 16]. It must be noted that these interactions are more pronounced in
 470 the composition with the ratio (1/2).



486 **Fig. 5** FTIR spectra of PVP and PPy in the 1500–1800 cm⁻¹ region.

486 Our results agree with those obtained previously with blends of polyaniline with polyvinylpyr-
 487 rolidone [17], poly (4-vinylphenol) and polyvinylmethylketone blends, and those reported by
 488 Belabed et al [18]. Similar observations have been also made by Kuo and coworkers in their
 489 study of blends of poly (vinylphenol-co-methyl methacrylate) with poly (ethylene oxide) [19].
 490 Although the qualitative study is relatively difficult in this region due to the overlapping be-
 491 tween the characteristic bands, we have attempted to study quantitatively using an appropriate
 492 curve fitting procedure.

493 The second step of this contribution is devoted to the quantification these interactions using the
 494 deconvolution methods in the range (1780-1630 cm⁻¹). The free and associated carbonyl frac-
 495 tions are also calculated by the following equation using an adequate curve fitting [20]:

$$f_{free}^{C=O} = \frac{A_{free}^{C=O}}{A_{free}^{C=O} + \alpha A_{Asso}^{C=O}} \quad (8)$$

497 where A is the peak areas corresponding to free and associated carbonyls and the absorptivity
 498 ratio (α) is assumed equal to 1.5. Table 3 summarizes the free and associated carbonyl fractions
 499 for the system PPy/PVP system. The careful examination of these fraction values indicates that
 500 the fraction of carbonyl bound associated to hydrogen decreases intimately with increasing the
 501 PVP content in the mixture, while that of free carbonyls remains almost constant. This is in
 502 good agreement with others works previously published [19]. Thus, we suggest that the hydro-
 503 gen bond interactions occurring between the amine /imine groups of PPy and the oxygen atom
 504 of PVP could be formed by breaking the hydrogen bond initially between PVP and water mol-
 505 ecules. However, the carbonyl stretching may certainly be affected by the presence of eventual
 506 hydrogen bond. In the other hand, we believe that the hydrogen bonded interactions occurred
 507 between PPy and PVP is more pronounced with the mixture in composition 1/1.

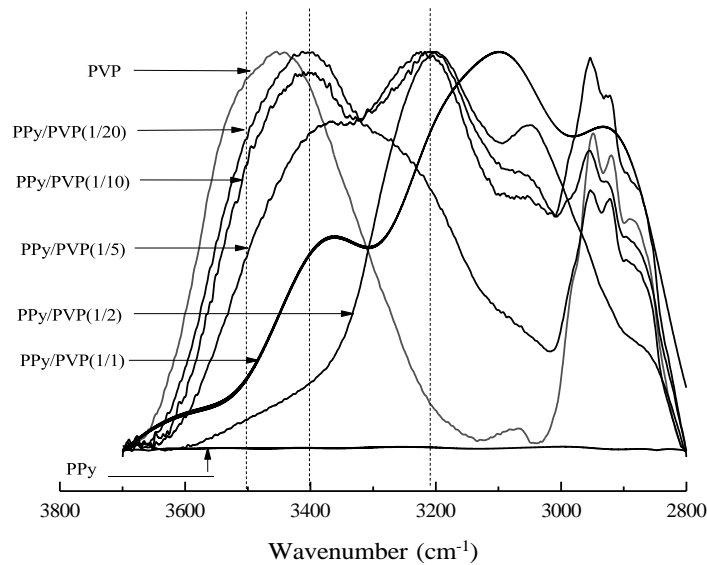
510 **Table 3** Curve fitting data from infrared spectra of PPy/PVP mixtures in the 1550-1750 cm⁻¹
 511 region.

| Blend composition | Free C=O | | | Hydrogen bonded C=O | | |
|-------------------|-----------------------|---------------------------|------------|-----------------------|---------------------------|------------|
| | Frequency | Width | Fraction | Frequency | Width | Fraction |
| PPy/PVP | $\nu(\text{cm}^{-1})$ | $w_{1/2}(\text{cm}^{-1})$ | f_{free} | $\nu(\text{cm}^{-1})$ | $w_{1/2}(\text{cm}^{-1})$ | f_{Asso} |
| 1/1 | 1650 | 18 | 0.641 | 1635 | 26 | 0.359 |
| 1/2 | 1651 | 20 | 0.523 | 1634 | 27 | 0.477 |
| 1/5 | 1648 | 21 | 0.427 | 1633 | 26 | 0.573 |
| 1/10 | 1651 | 22 | 0.278 | 1634 | 29 | 0.722 |
| 1/20 | 1650 | 19 | 0.259 | 1635 | 28 | 0.741 |

512
 513
 514 The FTIR spectra of PVP, PPy and their mixtures in the hydroxyl region are shown in Fig. 6.
 515 The spectrum of PVP exhibits three characteristic peaks at 3500, 3400 and 3260 cm⁻¹, assigned
 516 to stretching vibrations of free and associated hydroxyls, as well as to tertiary amine, respec-
 517 tively [17]. This phenomenon could be attributed to the hygroscopic nature of PVP, where the

518 nitrogen atom is adjacent to the carbonyl group in the PVP species, and which the water mole-
519 cules can be easily adsorbed by forming a hydrogen bridge.

520 Fig. 6 illustrates that as the PVP content in the thermoplastic matrix increases, the intensity of
521 the characteristic bands corresponding to the free hydroxyl groups of PVP, observed at 3453
522 cm^{-1} , progressively decreases and shifts to lower frequencies. This shift is likely attributed to
523 the disruption of self-association interactions.



535 **Fig. 6** FTIR spectra of PVP, PPy and their blends in the 2800–3800 cm^{-1} region

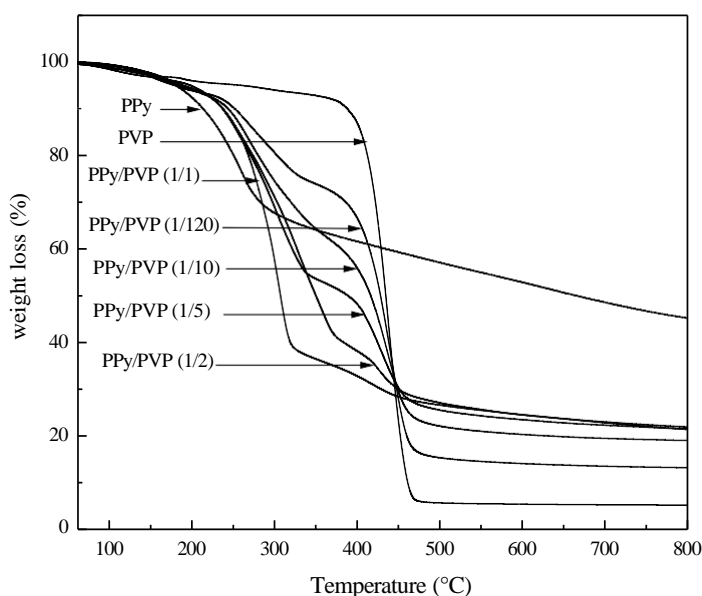
537 On the other way, a new band is detected at lower frequency (3220 cm^{-1}) confirming the pres-
538 ence of strong hydrogen bond between amine / imine groups with the carbonyl groups present
539 within PVP.

541 5. TGA Study

542 The thermal stability of polymers is a crucial property that defines their potential applications
543 and usage limits. During processing, polymeric materials are often exposed to relatively high
544 temperatures and pressures. Consequently, the study of the thermal behavior of synthesized
545 polymers and their blends continues to generate significant interest, as reflected in the numerous
546 studies published regularly [21, 22].

547 In order to determine the upper temperature limit of the processing and utilization these mate-
548 rials, the thermogravimetric analysis is widely used for the kinetic of the thermal degradation
549 and the possibility to form cross-linked structures. For these purposes, the TGA study is carried
550 out to get preliminary insights on the thermal stability of PPy combined with the thermoplastic
551 matrix of PVP. Fig. 7 displays the thermogravimetric curves for PPy, PVP and their mixture

552 obtained by in situ polymerization. It is seen that PPy shows a thermal stability up to 170 °C
553 above which the polymer degrades in two main stages of which the first, in the temperature
554 region (80-120 °C) consists of one minor step. The main loss in this region is assigned to the
555 elimination of water adsorbed by the hydrophilic groups. The second stage observed above 200
556 °C, is mainly attributed to the decomposition of the main chain by random scissions.



557
558 **Fig. 7.** TGA thermograms of PPy, PVP and their different ratios

559
560 However, despite the prolonged drying of this polymer under vacuum at 50 °C for several days,
561 traces of moisture still remain. Indeed, the weight loss varying from 2 to 20%, observed with
562 this polymer, in the range (90-150 °C), is attributed to the water molecules retained and possibly
563 to the traces of monomers or solvent trapped within the polymer chains. Overall, this polymer
564 exhibits significantly a better thermal stability compared to that of PPy. The onset of main deg-
565 radation is observed from 380 °C.

566 The addition of PVP within PPy substantially increases its thermal stability. It should be noted
567 that the mass losses recorded in the considered temperature range is notably decreases
568 notably with increasing of PVP composition in the mixture. This could be due, in part, to the
569 formation of specific hydrogen bond between the two polymers, as confirmed previously by
570 FTIR, the same thermal behaviour was observed in the polyaniline/polyvinylpyrrolidone mix-
571 ture [17]

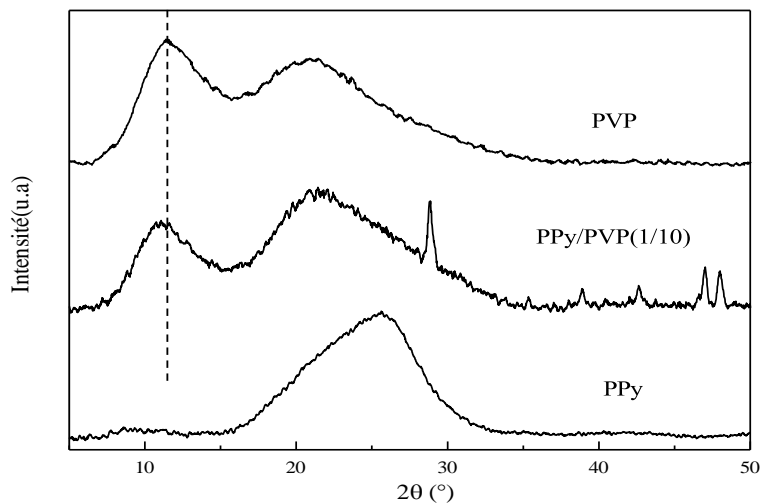
572

573 6. X-RD analysis

574 Fig. 8 shows the diffractograms of doped PPy powder, PVP films and their mixture (PPy/PVP:
575 1/10). The former has a broad band centred at 25.6° characteristic of the amorphous nature of
576 PPy [24]. On the other side, the amorphous morphology of PVP is illustrated by the presence
577 of two broad bands centred at 11.6 and 21.2°, respectively.

578 A comparison of the patterns shows that PPy has no peaks up to 15°. We can therefore use the
579 peak 11.6° of PVP to study the miscibility of PPy/PVP and this band is slightly shifted towards
580 lower 2θ angles indicating greater inter-reticular distances. This is due, partially, to the specific
581 interactions by ‘hydrogen bond’ between the two polymers. Similar results were found recently
582 for the ternary system “PPy/polyvinyl alcohol/chitosan blend” [25].

583 The XRD peaks (28.9°, 38,9°, 42.74°, 47°,48.1°) belong to inorganic salts resulting from the
584 synthesis of PPy using the persulfate $S_2O_8^{2-}$ which is reduced to SO_4^{2-} (Fig. 8). It is useful to
585 emphasize that the elimination of these salts requires several washes with distilled water for a
586 time not exceeding 1 h, otherwise swelling occurs due to the hygroscopic nature of the PVP
587 matrix.



598 **Fig. 8** X-ray diffraction patterns of PPy, PVP and PPy/PVP (1/10) blend.

602 7. Electrical conductivity and optical gap

603 The intrinsic conductivity of PPy is attractive in photoelectrochemistry [3] and has already been
604 explored since its discovery. It is due to alternating bonds ($\pi \rightarrow \pi^*$) of the benzenoid leading
605 to electronic delocalization with moderate carrier density [26].

606 All samples have a conductivity between 57 and 3960 $\mu S\ cm^{-1}$, a range belonging to the
607 semiconducting materials as expected, σ decreases with the film thickness and diminishes with

608 increasing the PVP amount in the mixture PPy/PVP, to reach its minimal value of 235 $\mu\text{S cm}^{-1}$
 609 for a ratio (PPy/PVP=1/20).

610

611 The PPy based materials are used in the solar energy conversion [3], and the knowledge of the
 612 gap (E_g) is crucial and is determined from the variation of the optical absorption coefficient ($\alpha\lambda$)
 613 with the photon energy ($h\nu$) using the well-known relation:

614

$$(\alpha h\nu)^n = K \times (h\nu - E_g) \quad (9)$$

616 K is a specific constant of the semiconductor and the exponent n indicates the nature of the
 617 optical transition, indirect (= 0.5) or direct (= 2). The values (Fig. 9) are obtained by extrapo-
 618 lating the lines $(\alpha h\nu)^2$ to the energy-axis and the transition is directly allowed.

619 The gap E_g and conductivity (σ) (Table 4) are correlated to each other. As we can see, the higher
 620 the conduction, the lower the gap, a predictable result. In addition, σ increases and E_g decreases
 621 with increasing the PPy percentage in the mixture PPy/PVP. This is due to a homogeneous
 622 dispersion of PPy on the PVP film with an increased active surface area; such property is
 623 attractive in photocatalysis [4] and similar results were obtained with the system PANI/PVP
 624 [17].

625 **Table 4** The Electrical conductivity and energy gap of different samples.

626

| Sample | σ (S cm^{-1}) $\times 10^5$ | E_g (eV) |
|----------------|---|------------|
| PPy | 5.70 | 0.80 |
| PPy/PVP (1/2) | 396 | 0.49 |
| PPy/PVP (1/5) | 212 | 0.50 |
| PPy/PVP (1/10) | 72.4 | 0.74 |
| PPy/PVP (1/20) | 23.5 | 0.77 |

627

628

629

630

631

632

1
2
3
4
5
6
7
8
9
10
11
12
13
14
15
16
17
18
19
20
21
22
23
24
25
26
27
28
29
30
31
32
33
34
35
36
37
38
39
40
41
42
43
44
45
46
47
48
49
50
51
52
53
54
55
56
57
58
59
60
61
62
63
64
65

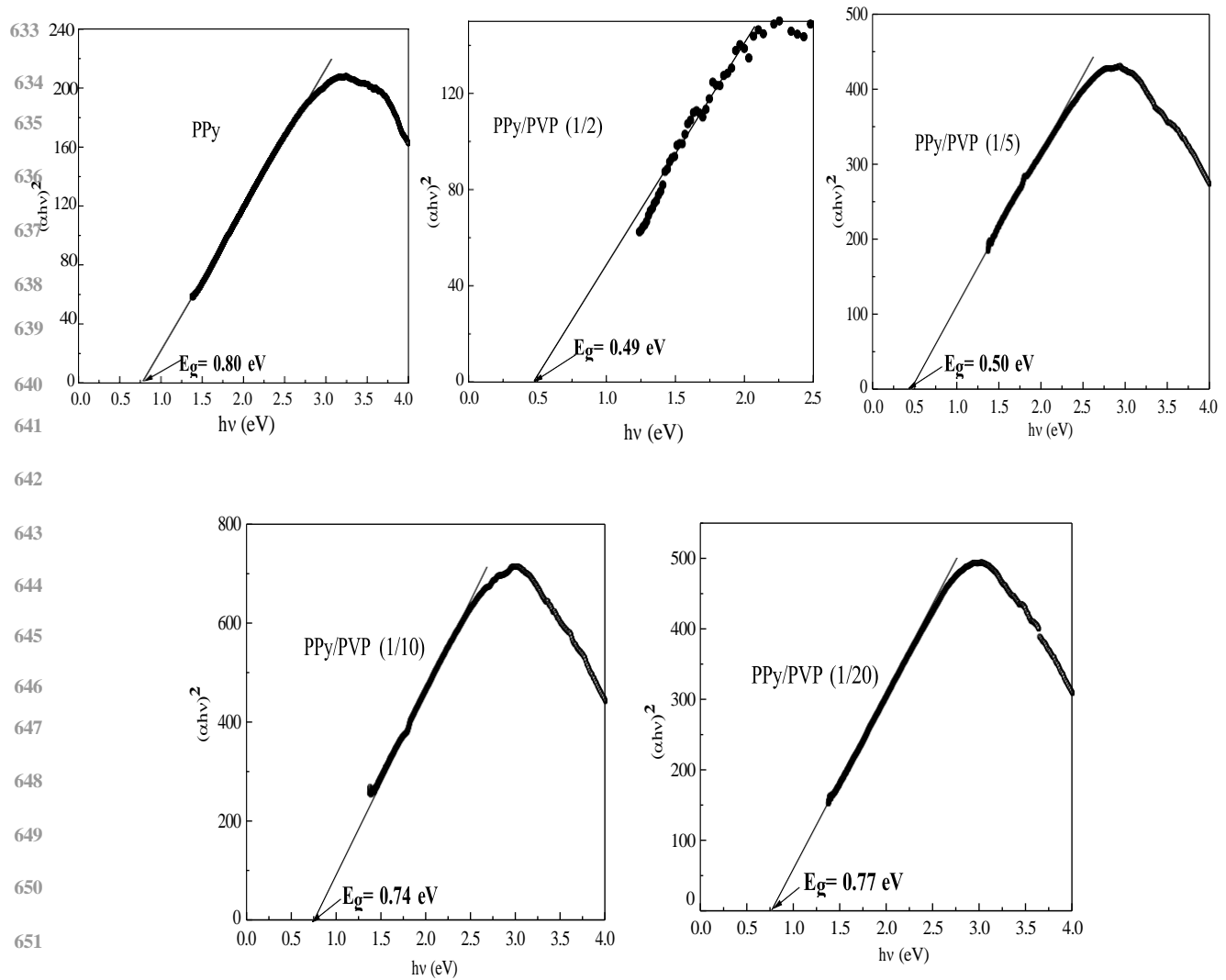


Fig. 9 Band gap transition of doped PPy and PPy/PVP mixtures at different ratios.

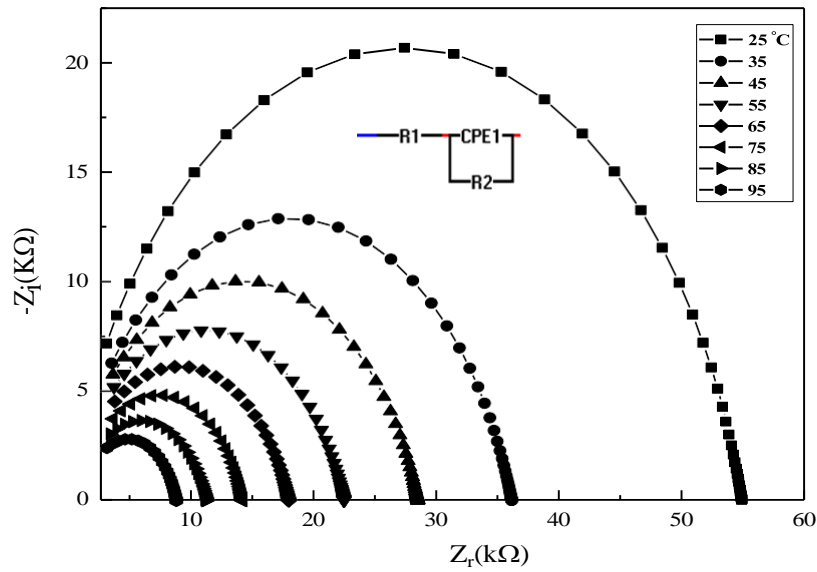
8. Electrical impedance

The impedance plots of doped PPy show large semicircles related to the bulk contribution whose diameter decreases with increasing temperature., thus supporting the semi conductivity (Fig. 10). The real axis gives the resistance of the sample and the non-existence right-hand semicircle indicates a weak contribution of grain boundaries. An equivalent electric circuit is suggested, consisting of the bulk resistance (R_b) in parallel with the capacity (C_b), the latter can be evaluated from the Bauerle' relation $\omega_p = 1/R_b C_b$ ω_p is the frequency at the top of the semicircle. The thermal variation of the electrical conductivity (σ) follows an exponential law Fig. 11.

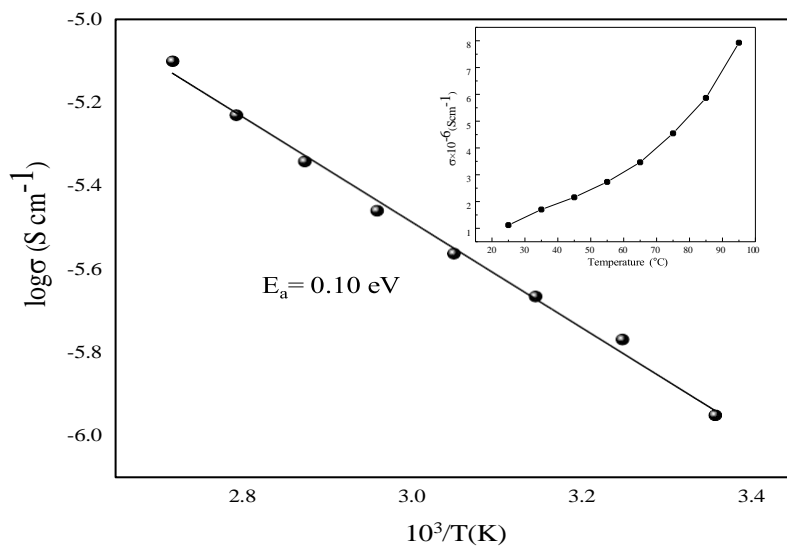
$$\sigma = e\mu N_A \tag{9}$$

where μ is the mobility of holes and N_A their density. The activation energy of doped PPy

667 (0.10 eV) determined from the slope ($d\log\sigma/dT^{-1}$), is close to that reported elsewhere (0.12 eV)
 668 [27]. This value is larger than the thermal energy kT (26 meV at 300 K) and this implies that
 669 both the mobility (μ) and density (N_A) are thermally activated at room temperature.



683 **Fig. 10** The EIS representation of doped PPy in the temperature range (25 - 95 °C). Inset: the
 684 equivalent electrical circuit.



698 **Fig. 11** Variation of the electrical conductivity (σ) of doped PPy versus $1/T$ (K)

702 Conclusions

1
2
3
4
5
6
7
8
9
10
11
12
13
14
15
16
17
18
19
20
21
22
23
24
25
26
27
28
29
30
31
32
33
34
35
36
37
38
39
40
41
42
43
44
45
46
47
48
49
50
51
52
53
54
55
56
57
58
59
60
61
62
63
64
65

703 In this study, we developed a series of semiconductor materials using in-situ polymerization,
704 based on polypyrrole (PPy) and polyvinylpyrrolidone (PVP). Initially, we optimized the
705 conditions for synthesizing pure PPy. These conditions were then applied to synthesize the
706 PPy/PVP heterosystem.

707
708 In this context, we assessed the optimal conditions to ensure their total miscibility using
709 thermodynamic considerations based on the group contributions method. By applying this
710 method, we calculate the solubility parameters of the two considered polymers. The results
711 indicate that complete miscibility occurs when the solubility parameters of the two polymers
712 are very closely.

713
714 The DSC and DMA analyses confirmed the miscibility of all PPy/PVP mixtures through the
715 observation of a single glass transition temperature (T_g).

716
717 The FTIR study shows the presence of specific intercatons of the hydrogen bond between the
718 unlike groups present towards the two polymers; amine and imine in PPy and carbonyl in PVP.
719 These interactions are evidenced by a shift of the free carbonyl band centered at 1652 cm^{-1}
720 towards lower wavelengths with increasing the PVP composition in the mixture, and the
721 observation of a new band at 1622 cm^{-1} , characteristic at the associated carbonyl.

722 The presence of hydrogen bond in different mixtures is also highlighted by quantitative analysis
723 in which the fraction of free and associated carbonyl in the corresponding regions was
724 estimated.

725 The XRD study of the PPy/PVP mixture shows that the peak 11.6° characteristic of PVP shifts
726 slightly toward lower 2θ angles indicating a greater inter-reticular distance. This is due,
727 partially, to the specific interactions that occurred between unlike species of two polymers.

728
729 The thermogravimetric analysis (TGA) of the various PPy/PVP materials demonstrated
730 enhanced thermal stability. The incorporation of PVP into PPy not only increases its thermal
731 stability but also alters the degradation process. This improvement can be attributed to the
732 excellent dispersion of PPy within the PVP matrix and the strong intermolecular interactions
733 formed between the two polymers.

734 Additionally, the thermal stability of the synthesized materials was significantly enhanced.

735

1
2
3
4
5
6
7
8
9
10
11
12
13
14
15
16
17
18
19
20
21
22
23
24
25
26
27
28
29
30
31
32
33
34
35
36
37
38
39
40
41
42
43
44
45
46
47
48
49
50
51
52
53
54
55
56
57
58
59
60
61
62
63
64
65

736 The optical gap of PPy in the mixture PPy/PVP determined by UV-Visible spectrophotometry
737 is attributed to $\pi \rightarrow \pi^*$ transition while, the electric conductivity, measured by the four-point
738 method reveal a semiconducting behaviour.

739 Electrochemical impedance spectroscopy (EIS) exhibits semicircles attributed to bulk material,
740 whose diameter decreases with increasing temperature, thus confirming the semiconducting
741 behavior of PPy; The data obey to an Arrhenius law with an activation energy of 0.1 eV and
742 the conduction occurs by electrons delocalization though alternating double bonds.

743

744 **Acknowledgements**

745

746 K. Zeggagh acknowledges the support of the Algerian Research Agency (DGRSDT): Project
747 B00L01UN160420220013).

748 **Conflict of interest:** The authors declare that they have no conflict of interest.

749

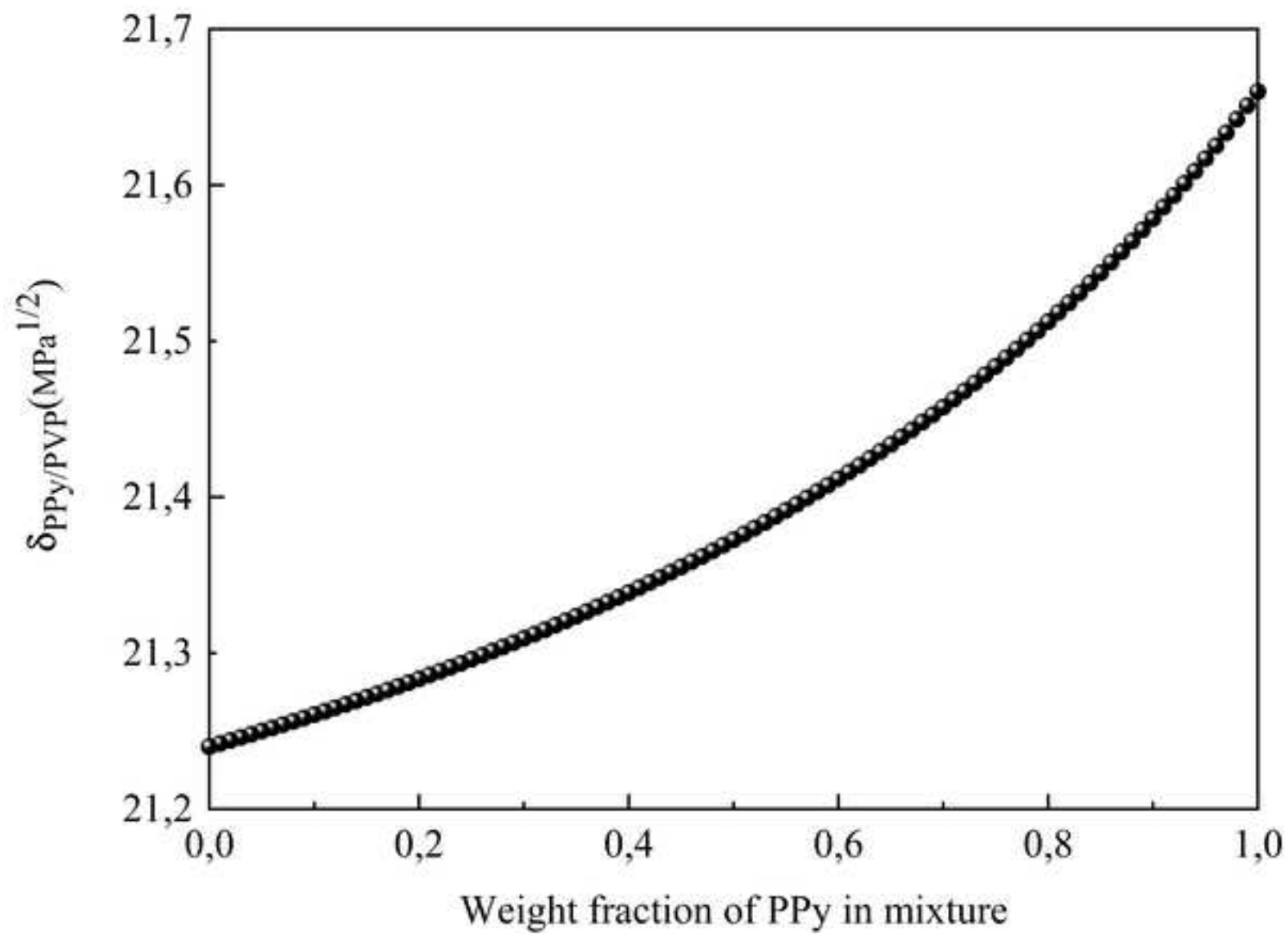
750 **Reference**

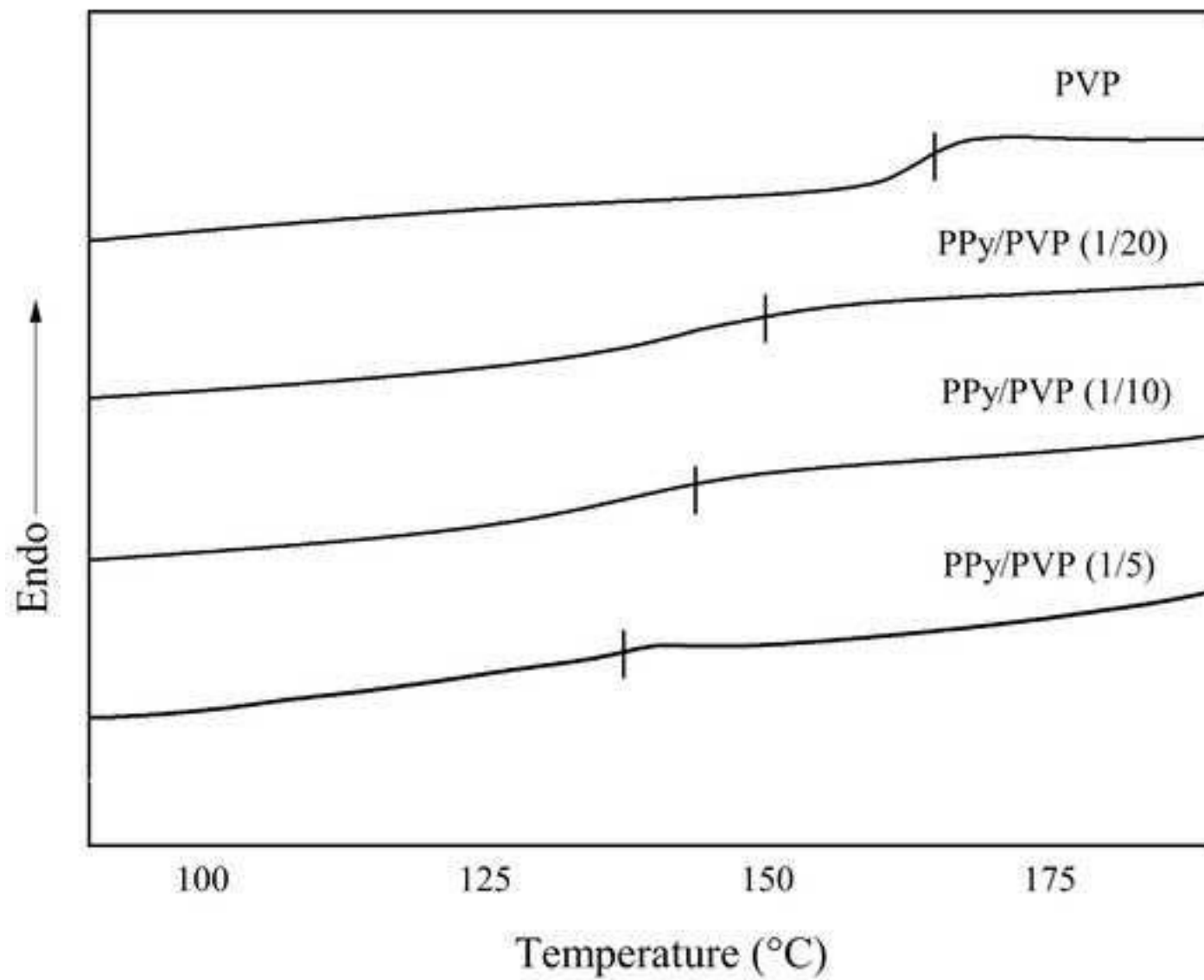
751

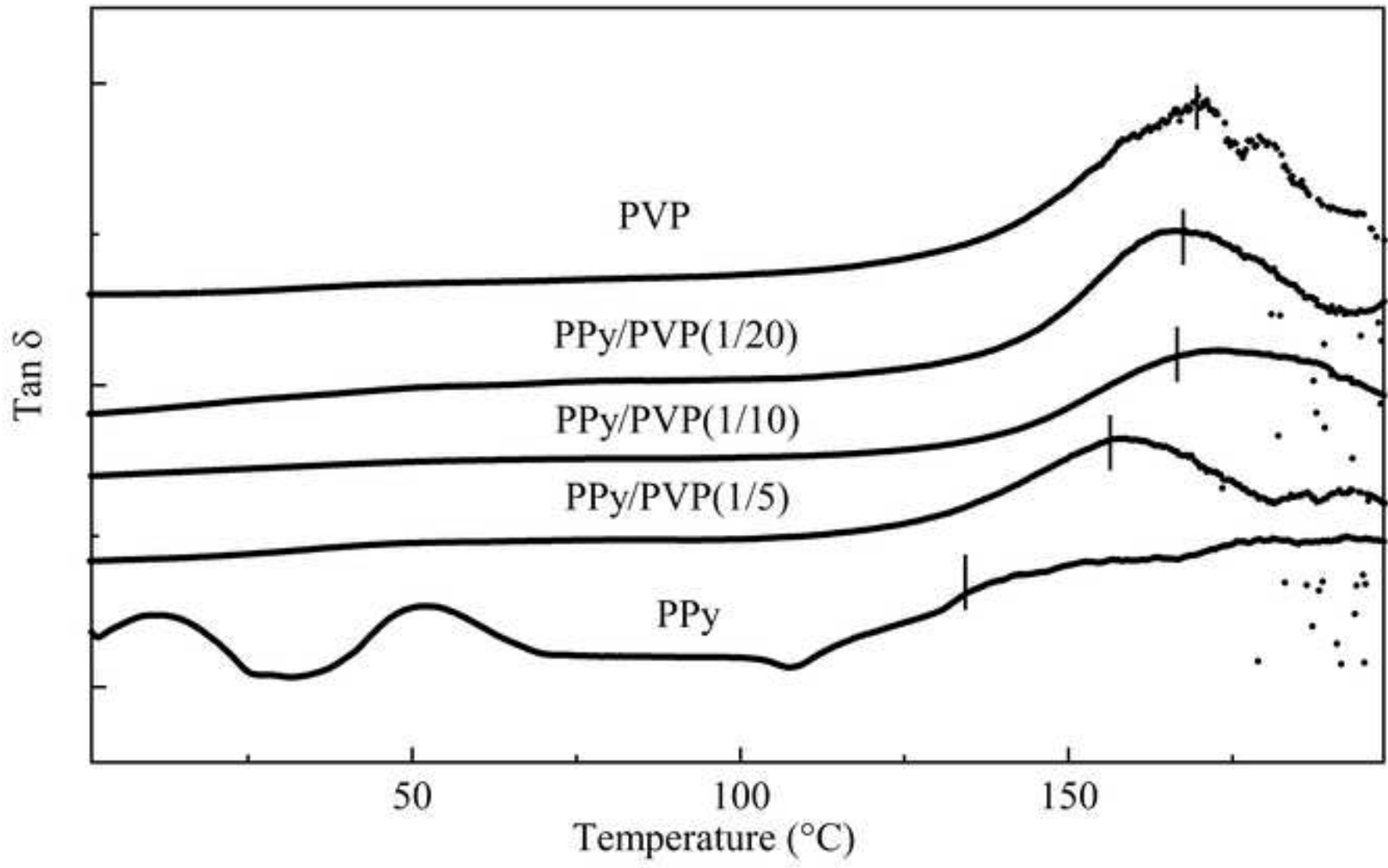
- 752 1. Wang X, Liu Q, Wu S, Xu B, Xu H. (2019) Multilayer polypyrrole nanosheets with self-
753 organized surface structures for flexible and efficient solar–thermal energy conversion.
754 *Advanced Materials* 31(19): 1807716.
- 755 2. Hao L, Dong C, Zhang L, Zhu K, Yu D. (2022) Polypyrrole nanomaterials: Structure, prep-
756 aration and application. *Polymers* 14(23): 5139.
- 757 3. Belabed CH, Gharib R, Merzak D, Benaldelghani Z, Trari M. (2013) Photo-electrochemi-
758 cal characterization of polypyrrole: Application to visible light induced hydrogen produc-
759 tion. *Sol Energy Mater Sol Cells* 114 :199–204.
- 760 4. Belabed Ch, Abdi A, Benabdelghani Z, Rekhila G, Etxeberria A, Trari M. (2013) Photoe-
761 lectrochemical properties of doped polyaniline: Application to hydrogen photoproduction.
762 *Int J Hydrogen Energy* 38 :6593–5699.
- 763 5. Chang CH, Huang TC, Peng CW, Yeh TC, Lu H-I, Hung W-I, Yeh J-M. (2012) Novel
764 anticorrosion coatings prepared from polyaniline/graphene composites. *Carbon* 50 :5044–
765 5051.
- 766 6. Anwar ulhaq AS, Akhlaq S, Sayed M, et al. (2018) Synthesis and characterization of pol-
767 yaniline–zirconium dioxide and polyaniline–cerium dioxide composites with enhanced
768 photocatalytic degradation of rhodamine B dye. *Chem Pap* 72 :2523–2538.

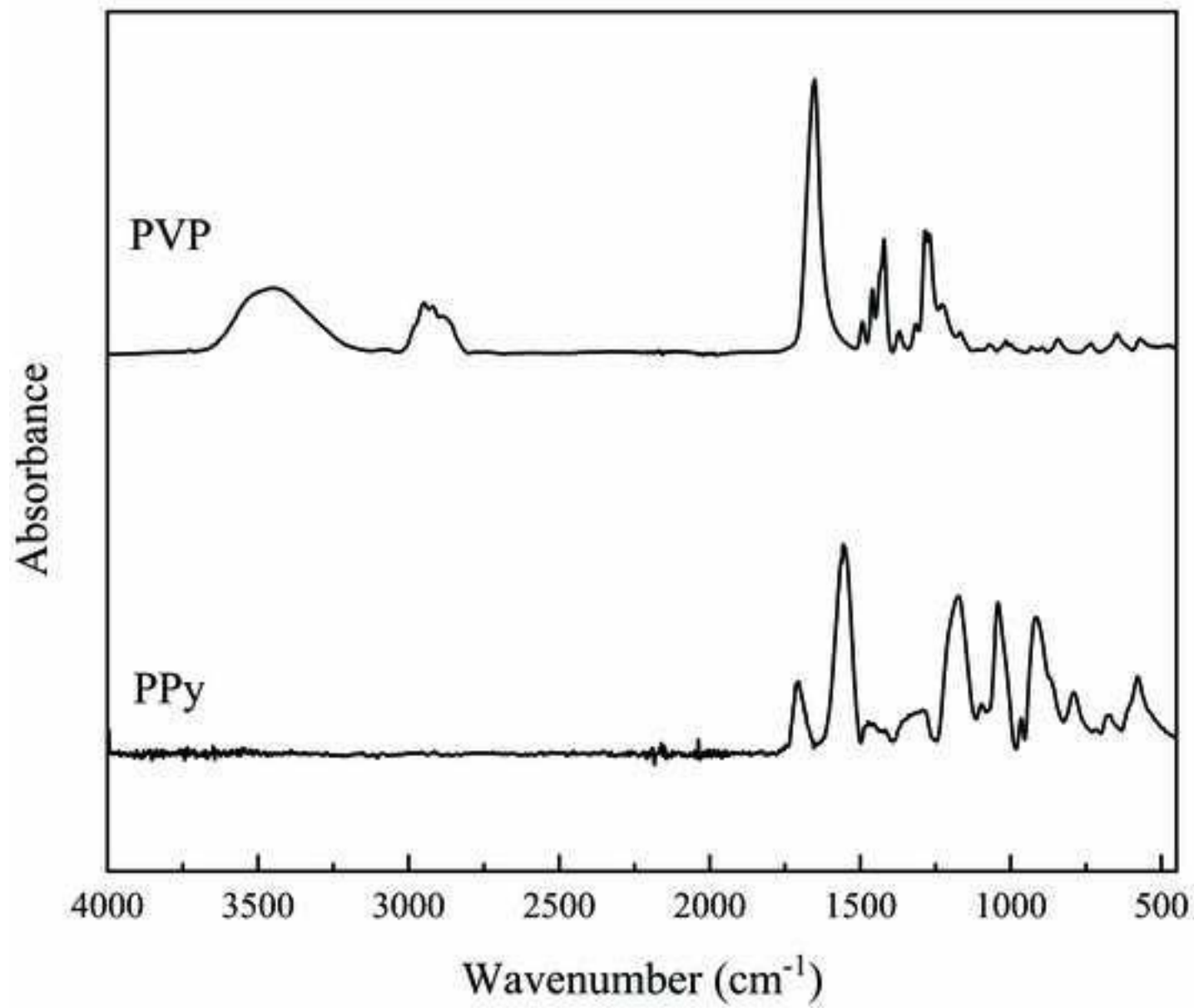
- 1
2
3
4
5
6
7
8
9
10
11
12
13
14
15
16
17
18
19
20
21
22
23
24
25
26
27
28
29
30
31
32
33
34
35
36
37
38
39
40
41
42
43
44
45
46
47
48
49
50
51
52
53
54
55
56
57
58
59
60
61
62
63
64
65
- 769 7. Shacklette LW. (1994) Dipole and hydrogen bonding interactions in polyaniline: a mechanism for conductivity enhancement. *Synth Met* 65 :123–130.
 - 770
771 8. Zaghlol S, Amer WA, Shaaban MH et al. (2020) Conducting macroporous polyaniline/poly(vinyl alcohol) aerogels for the removal of chromium(VI) from aqueous media. *Chem Pap* 74 :3183–3193.
 - 772
773
774 9. Jahangir S, Ali Reza Z, (2020) Electrochemically imprinted self-doped polyaniline as highly sensitive voltametric sensor for determination of bismuth in water, wastewater, and pharmaceutical samples, *Journal of Mater Sci*: doi.org/10.1007/s10337-019-03841-7
 - 775
776
777 10. Coleman MM, Graf JF, Painter PC. (1991) *Specific Interactions and the Miscibility of Polymer Blends*; Technomic Publishing: Lancaster. PA, USA.
 - 778
779 11. Hansen CM, Beerbower A. (1971) Solubility parameters. In *Kirk Othmer Encyclopedia of Chemical Technology*, Suppl. Vol., 2nd ed.; Standen, A., Ed.; Interscience: New York.
 - 780
781 12. Van Krevelen DW, te Nijenhuis KU. (2009) *Properties of Polymers: Their Correlation with Chemical Structure: Their Numerical Estimation and Prediction from Additive Group Contributions*. Elsevier Science, New York.
 - 782
783
784 13. Ballard G, Al-Saigh Z. Y., (2019) Solubility and Surface Thermodynamics of Conducting Polymers by Inverse Gas Chromatography, IV: Polypyrrole/Titanium Oxide, *Chromatographia*: doi.org/10.1007/s10337-019-03841-7.
 - 785
786
787 14. Heidi R, Painter PC, Coleman MM. (2001) Interactions in miscible blends of poly(styrene-co-methacrylic acid) with copolymers containing vinylpyrrolidone and vinylpyridine groups. *Macromolecules* 34:8390–8393.
 - 788
789
790 15. Hazarika J, Kumar A. (2016) Structural and optical properties of self-assembled polypyrrole nanotubes. *Journal of Polymer Research* 23: 1-8.
 - 791
792 16. Omastová M, Trchová M, Kovářová J, Stejskal J. (2003) Synthesis and structural study of polypyrroles prepared in the presence of surfactants. *Synthetic metals* 138(3): 447-455.
 - 793
794 17. Atia S, Zeggagh K, Hadjout S, Etxeberria A, Benabdelghani Z. (2022) Enhancement of semiconducting and thermomechanical properties of materials based on polyaniline and polyvinylpyrrolidone. *Journal of Polymer Research* 29(4): 138.
 - 795
796
797 18. Belabed CH, Benabdelghani Z, Granado A, Etxeberria A. (2012) Miscibility and specific interactions in blends of poly(4-vinylphenol-co-methyl methacrylate)/poly(styrene-co-4-vinylpyridine). *J Appl Polym Sci* 125:3811–3819.
 - 798
799
800 19. Shiao WK, Chang FC. (2001) Miscibility and hydrogen bonding in blends of poly(vinylphenol-co-methyl methacrylate) with poly(ethylene oxide). *Macromolecules* 34 :4089–4097.
 - 801
802

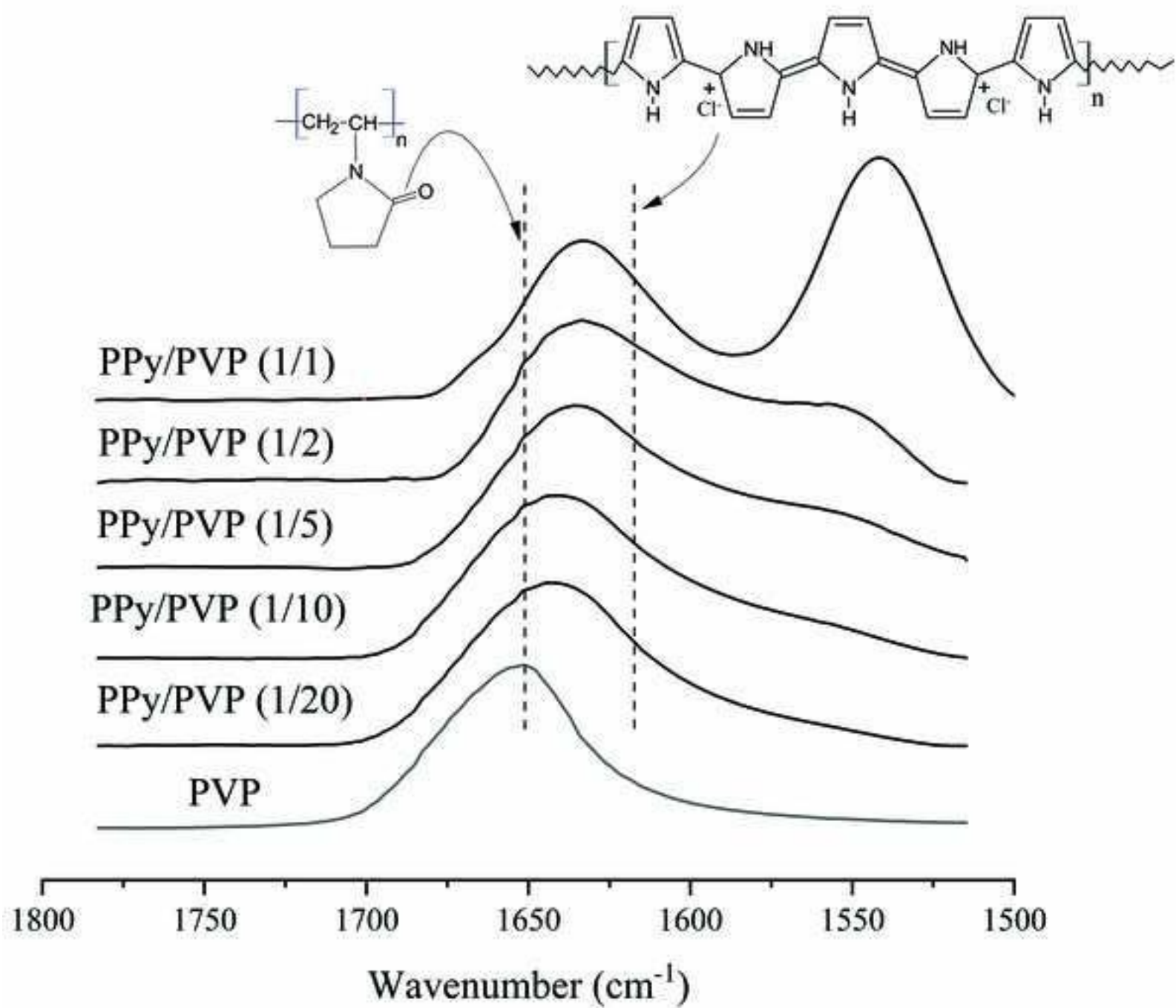
- 1
2
3
4
5
6
7
8
9
10
11
12
13
14
15
16
17
18
19
20
21
22
23
24
25
26
27
28
29
30
31
32
33
34
35
36
37
38
39
40
41
42
43
44
45
46
47
48
49
50
51
52
53
54
55
56
57
58
59
60
61
62
63
64
65
- 803 20. Shiao WK, Chang FC. (2001) Studies of miscibility behavior and hydrogen bonding in
804 blends of poly(vinylphenol) and poly(vinylpyrrolidone). *Macromolecules* 34 :5224–5228.
- 805 21. Yahong Z, Yuping D, Liu Jia, Guojia M, Mingliang H. (2018) Wormlike acid-doped pol-
806 yaniline: controllable electrical properties and theoretical investigation. *J Phys Chem C*
807 122(4):2032–2040.
- 808 22. Bourara H, Hadjout S, Benabdelghani Z, Etxeberria A. (2014) Miscibility and Hydrogen
809 Bonding in Blends of Poly(4-vinylphenol)/Poly(vinyl methyl ketone). *Polymers* 6:2752–
810 2763.
- 811 23. Benabdelghani Z, Etxeberria A. (2011) The phase behavior and thermal stability of blends
812 of poly(styrene-co-methacrylic acid)/poly(styrene-co-4-vinylpyridine). *J Appl Polym Sci*
813 121 :462–468.
- 814 24. Tejskal J. (2020) Interaction of conducting polymers, polyaniline and polypyrrole, with
815 organic dyes: polymer morphology control, dye adsorption and photocatalytic decomposi-
816 tion. *Chem Pap* 74 :1–54.
- 817 25. Irfan M, Shakoor A. (2019) Structural Electrical and Dielectric Properties of Dodecylben-
818 zene Sulphonic Acid Doped Polypyrrole/Nano-Y. *Journal of Inorganic and Organometallic*
819 *Polymers and Materials* 30:1287–1292.
- 820 26. Eisa WH et al. (2016) PVP induce self-seeding process for growth of Au@ Ag core@ shell
821 nanocomposites. *Chemical Physics Letters* 651: 28-33.
- 822 27. Elashmawi IS, Ismail AM, Abdelghany AM. (2023) The incorporation of polypyrrole
823 (PPy) in CS/PVA composite films to enhance the structural, optical, and the electrical con-
824 ductivity. *Polymer Bulletin* 80: 11379-11399.

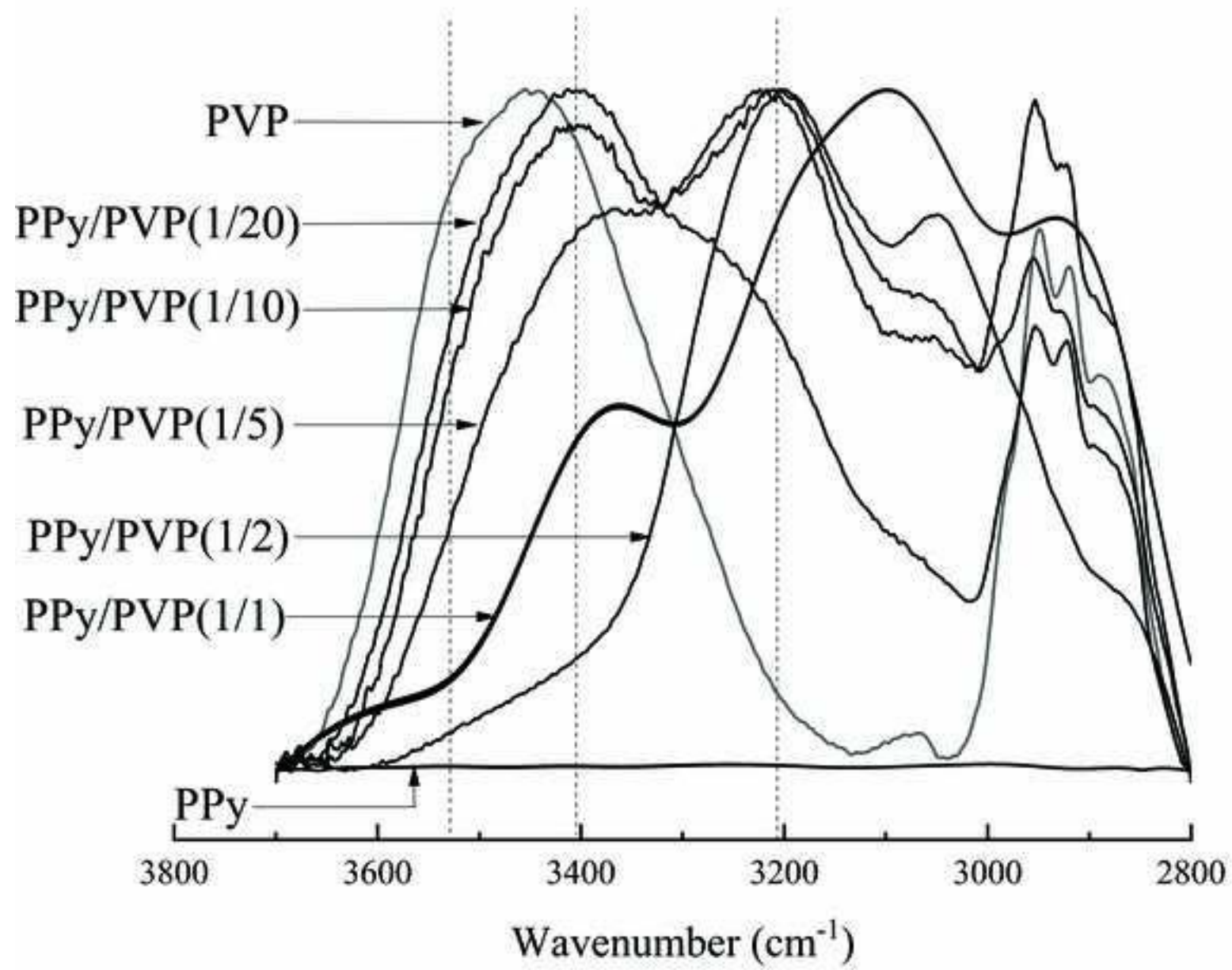


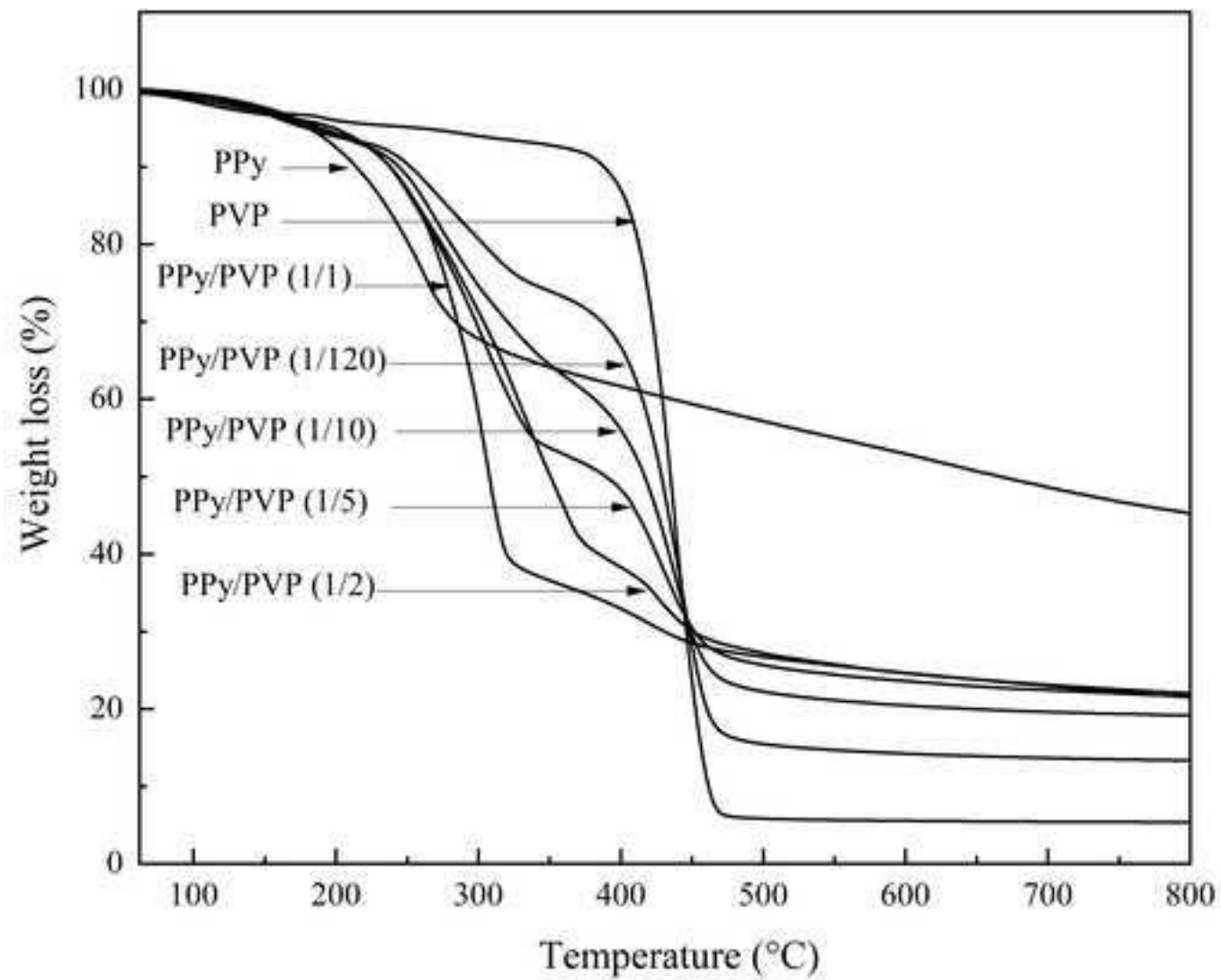


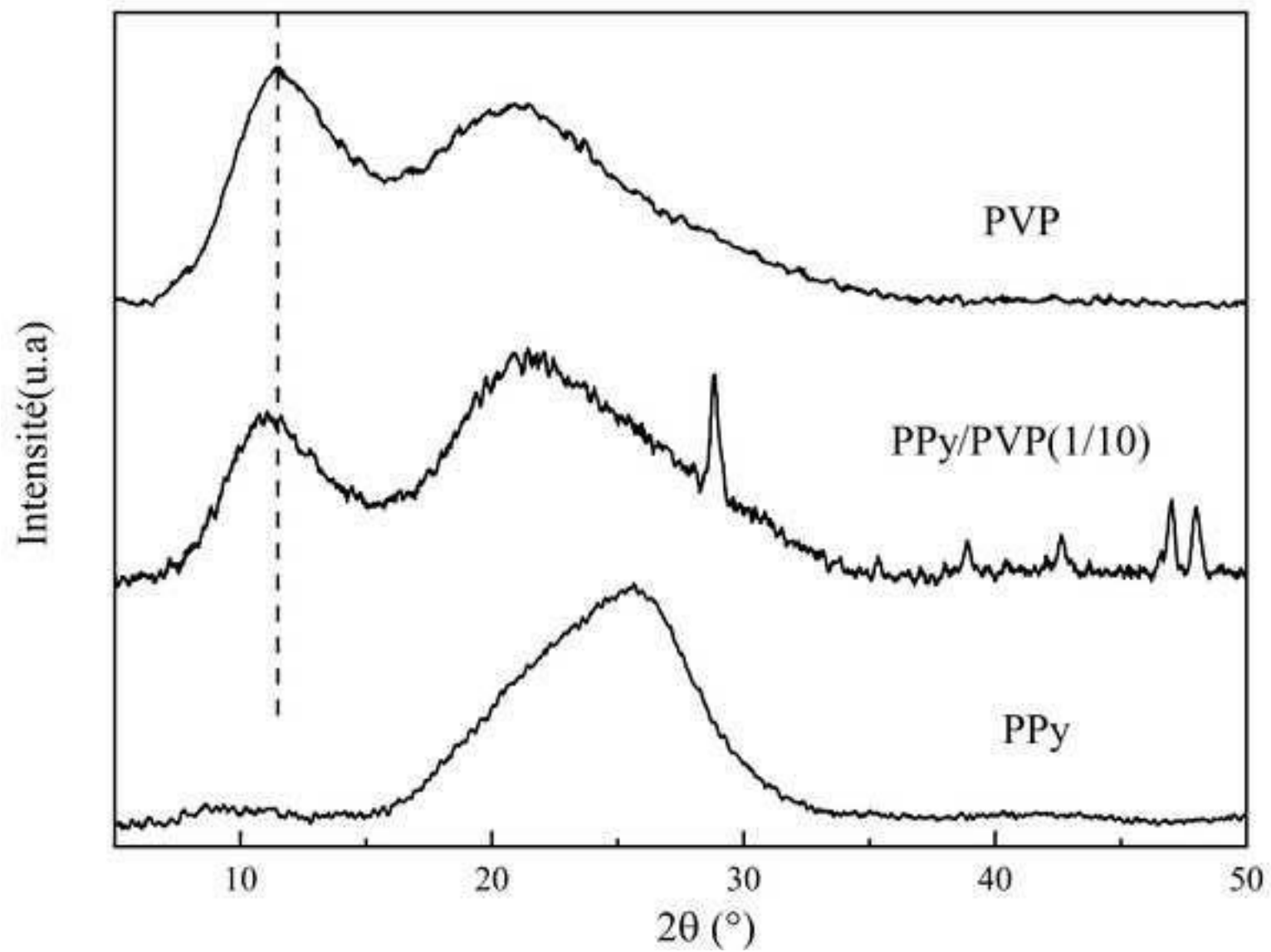


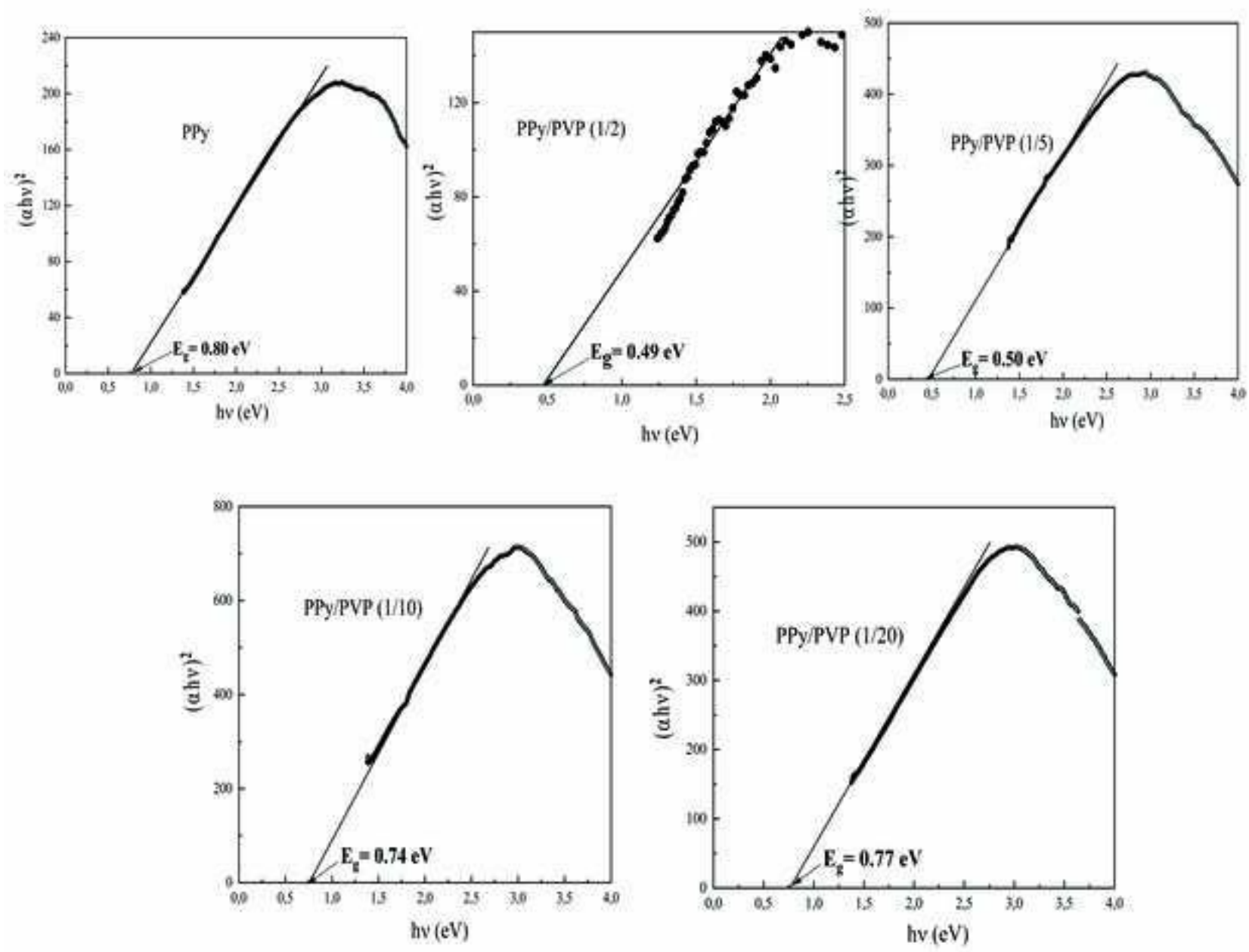












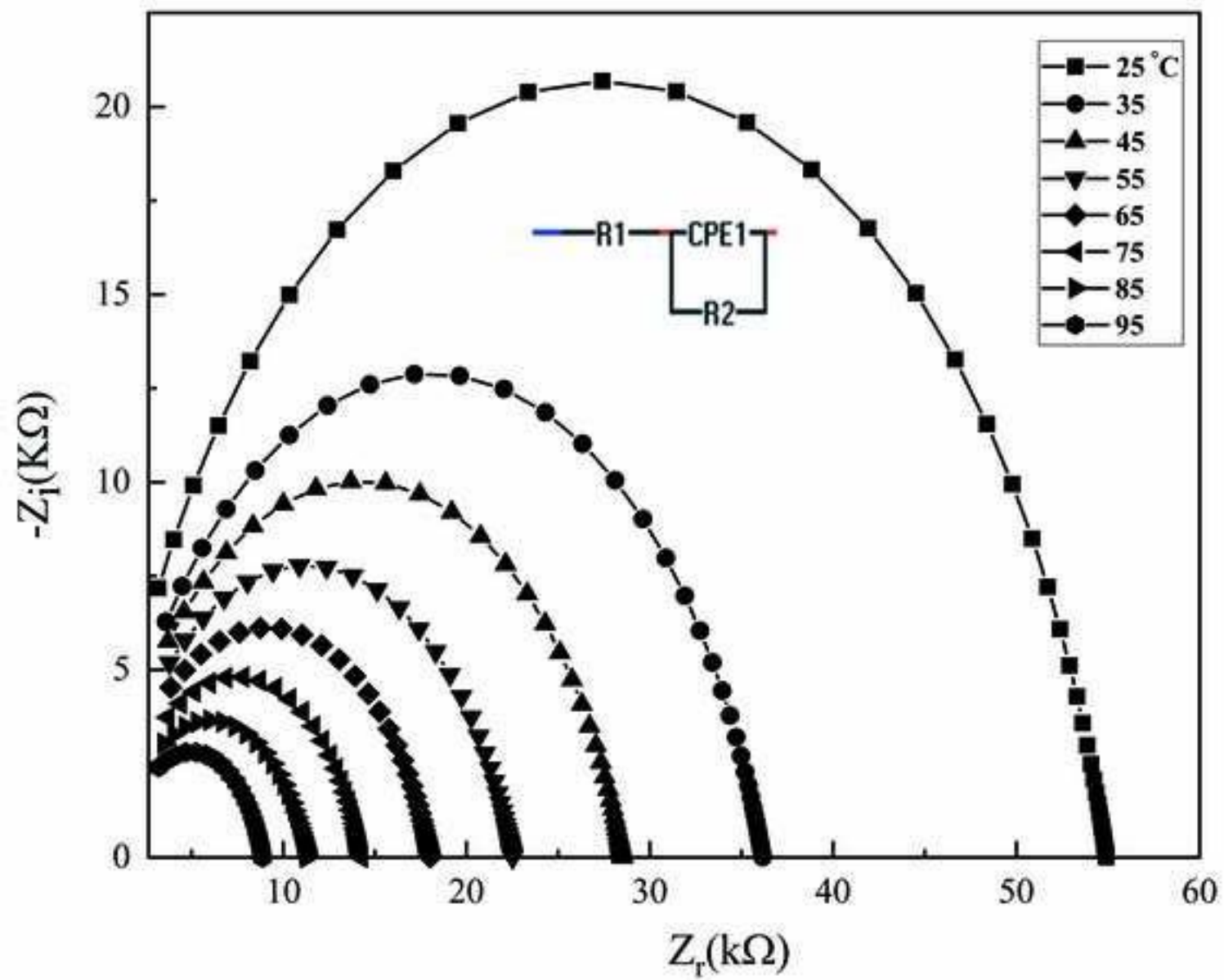


Table 1. Polymerization conditions of pure PPy and PPy/PVP blend at different ratios.

| Composition of Pyrrole/PVP | Pyrrole (mL) | HCl 1M (mL) | (NH ₄) ₂ S ₂ O ₈ (g) | PVP (g) |
|-------------------------------|-----------------|----------------|--|------------|
| 1/0 | 1 | 21.68 | 3.79 | - |
| 1/1 | 0.5 | 10.84 | 1.90 | 0.61 |
| 1/2 | 0.5 | 10.84 | 1.90 | 1.21 |
| 1/5 | 0.5 | 10.84 | 1.90 | 3.03 |
| 1/10 | 0.5 | 10.84 | 1.90 | 6.06 |
| 1/20 | 0.2 | 4.33 | 0.76 | 4.84 |

Table 2 Predicted solubility parameters of PVP and PPy using group contributions theory

| Polymers | δ_t | δ_d | δ_p | δ_h |
|----------|------------|------------|------------|------------|
| PVP | 21.24 | 15.50 | 11.70 | 08.60 |
| PPy | 21.66 | 19.50 | 04.60 | 08.24 |

Table 3 Curve fitting data from infrared spectra of PPy/PVP mixtures in the 1550-1750 cm^{-1} region.

| Blend composition | Free C=O | | | Hydrogen bonded C=O | | |
|-------------------|-----------------------|---------------------------|-------------------|-----------------------|---------------------------|-------------------|
| | Frequency | Width | Fraction | Frequency | Width | Fraction |
| PPy/PVP | $\nu(\text{cm}^{-1})$ | $w_{1/2}(\text{cm}^{-1})$ | f_{free} | $\nu(\text{cm}^{-1})$ | $w_{1/2}(\text{cm}^{-1})$ | f_{Asso} |
| 1/1 | 1650 | 18 | 0.641 | 1635 | 26 | 0.359 |
| 1/2 | 1651 | 20 | 0.523 | 1634 | 27 | 0.477 |
| 1/5 | 1648 | 21 | 0.427 | 1633 | 26 | 0.573 |
| 1/10 | 1651 | 22 | 0.278 | 1634 | 29 | 0.722 |
| 1/20 | 1650 | 19 | 0.259 | 1635 | 28 | 0.741 |

Table 4 The electrical conductivity and energy gap of different samples.

| Sample | σ (S cm ⁻¹) $\times 10^5$ | E _g (eV) |
|----------------|--|---------------------|
| PPy | 5.70 | 0.80 |
| PPy/PVP (1/2) | 396 | 0.49 |
| PPy/PVP (1/5) | 212 | 0.50 |
| PPy/PVP (1/10) | 72.4 | 0.74 |
| PPy/PVP (1/20) | 23.5 | 0.77 |